Mathematical Biosciences 331 (2021) 108501

Contents lists available at ScienceDirect

Mathematical Biosciences

journal homepage: www.elsevier.com/locate/mbs

Original Research Article

Spatial modeling and dynamics of organic matter biodegradation in the absence or presence of bacterivorous grazing☆

Xiaoyuan Chang [a], Junping Shi [b,*], Hao Wang [c]

[a] Department of Mathematics, Harbin University of Science and Technology, Harbin, Heilongjiang, 150080, PR China
[b] Department of Mathematics, William & Mary, Williamsburg, VA, 23187-8795, USA
[c] Department of Mathematical and Statistical Sciences, University of Alberta, Edmonton, Alberta, T6G 2G1, Canada

ARTICLE INFO

MSC:
92D25
92C70
35K57
35B32
35B40

Keywords:
Biodegradation
Reaction–diffusion
Bifurcation
Persistence
Organic matter decomposition
Bacteria
Grazer
Stoichiometric model
Carbon
Nitrogen

ABSTRACT

Biodegradation is a pivotal natural process for elemental recycling and preservation of an ecosystem. Mechanistic modeling of biodegradation has to keep track of chemical elements via stoichiometric theory, under which we propose and analyze a spatial movement model in the absence or presence of bacterivorous grazing. Sensitivity analysis shows that the organic matter degradation rate is most sensitive to the grazer's death rate when the grazer is present and most sensitive to the bacterial death rate when the grazer is absent. Therefore, these two death rates are chosen as the primary parameters in the conditions of most mathematical theorems. The existence, stability and persistence of solutions are proven by applying linear stability analysis, local and global bifurcation theory, and the abstract persistence theory. Through numerical simulations, we obtain the transient and asymptotic dynamics and explore the effects of all parameters on the organic matter decomposition. Grazers either facilitate biodegradation or has no impact on biodegradation, which resolves the "decomposition–facilitation paradox" in the spatial context.

1. Introduction

As one of the major global crises, environmental pollution has received much attention all over the world. According to the sixth global environment outlook report issued by the United Nations Environment Programme during the United Nations Environment Conference in March 2019, pollution of the earth's environment is severe and the risk to human health is increasing every day. A friendly way of decomposing environmental pollutants is to use microbial decomposers, such as bacteria, who can degrade organic matters composed of different elements including carbon, nitrogen, sulfur and phosphorus [1]. This process is called biodegradation during which, certain substances are decomposed into natural elements by microorganisms. Microbial biodegradation is a natural recycling process and is beneficial in both environmental and economic perspectives [2].

Bacteria are one of the most numerous and oldest living creatures on the earth. Bacteria and their predators (e.g. protists) play indispensable roles in the sustainability and restoration of natural ecosystems. They significantly impact biodegradation of organic matters. Hence, it is useful and interesting to explore the dynamics of biodegradation using stoichiometric modeling which provides a cutting–edge approach to study macroscopic phenomena (organic matters from pollution and their decomposition) via microscopic lens (bacteria, protists, carbon and nitrogen elements) [3–5].

In [5], Wang et al. established a bacteria–grazer model of organic matter decomposition and revealed the positive relationship between the facilitation of organic matter decomposition by grazers and the stoichiometric difference between bacteria and grazers by using numerical simulations. They also term the "decomposition–facilitation paradox" phenomenon, which points out that the rate or the extent of organic matter decomposition often increases in the presence of bacterivorous protists that substantially reduce bacterial abundances; see also [6–10]. Based on the model in [5], the authors in [4] studied the dynamics of a stoichiometric organic matter decomposition model in chemostat under the "well stirred" assumption which is the case in

☆ X. Chang is supported by NSFC, PR China-11901140, NSFHLJ, PR China-A2018009, J. Shi is partially supported by National Science Foundation, USA DMS-1853598, and H. Wang is partially supported by NSERC, Canada RGPIN-2020-03911 and RGPAS-2020-00090.

* Corresponding author.
E-mail address: jxshix@wm.edu (J. Shi).

https://doi.org/10.1016/j.mbs.2020.108501
Received 22 June 2020; Received in revised form 29 September 2020; Accepted 26 October 2020
Available online 6 November 2020
0025-5564/© 2020 Elsevier Inc. All rights reserved.

many lab experiments. These well-mixed ODE models were modified and applied to estimate methane production from oil sands industry in Alberta province of Canada [3]. Lab experiments were designed for the methane emission model to guarantee the rationality of the "well stirred" assumption. However, in natural ecosystems, the decomposition usually occurs in a spatially heterogeneous media. Therefore, we propose a reaction–diffusion PDE model for the stoichiometric organic matter decomposition (see Section 2) by extending the kinetic equations in [4] to the setting of an unstirred media in this paper.

Through analyzing and simulating the reaction–diffusion PDE model, our main conclusions include the following:

(i) If the bacterial death rate ϵ is greater than a threshold ϵ^*, then the bacteria always go extinct regardless of the grazer presence; On the other hand, the bacteria persist when the death rate is smaller than the threshold.
(ii) If the bacteria death rate ϵ is smaller than the threshold ϵ^* and the grazer death rate β is smaller than a threshold β^*, then the grazer and bacteria both persist and they reach a coexistence steady state.
(iii) When both of the grazer and bacteria persist, increasing the carbon input rate destabilizes the grazer–bacteria coexistence steady state and a spatial–temporal oscillatory pattern emerges. Thus a paradox of enrichment occurs as in the classical predator–prey system, that is, increasing the food available to the prey can cause a destabilization of the predator's population in a predator–prey model [11].
(iv) Sensitivity analysis of the degradation rate to the parameters reveals that the presence of grazers facilitates the organic matter decomposition, which explains the "decomposition–facilitation paradox" in the spatially heterogeneous context. The increase of the flow rate, although enhances the decomposition, reduces grazers' facilitation, and sufficiently large flow exchange makes the decomposition rate same in the presence or absence of grazers. The effects of other parameters on the grazers' facilitation are also studied.

The conclusions (i) and (ii) are rigorously proven using the linear stability theory, the local and global bifurcation theory and the abstract persistence theory. The conclusions (iii) and (iv) are obtained by numerical simulations.

Our paper is organized as follows. We present our model in Section 2 and provide some mathematical preliminaries in Section 3. In Section 4, the dynamical behaviors of the grazer–absent system are obtained. The main results of the dynamical properties of the grazer-present system are stated and proven in Section 5. Numerical simulations in Section 6 validate our mathematical results in Section 4 and Section 5, and transient and permanent oscillatory behavior are also found numerically. Sensitivity analysis is also included in Section 6. We summarize and discuss our outcomes in Section 7. All technical proofs of mathematical results are given in the Appendix.

2. The model

Our model is based on the model in [4] and describes the life cycle that bacteria decompose the organic matter, bacterivorous grazers graze the bacteria and the organic matter recycle from dead bacteria and grazers in an unstirred media. The spatial domain is assumed to be a one-dimensional tubular reactor $0 < x < L$. Here, similar to the assumptions in [5], the organic matter is the combination of organic carbon and organic nitrogen, and organic nitrogen in organic matter and inorganic nitrogen are combined together as the available nitrogen pool. We use organic carbon decomposition as a proxy for organic matter decomposition and assume that bacteria and bacterivorous grazers biomass are in terms of carbon content [12].

Our model has four state variables: the concentration of bacterial biomass measured in carbon $B(x,t)$, the concentrations of carbon $C(x,t)$ and nitrogen $N(x,t)$ in media, and the concentration of grazers $G(x,t)$ predating bacteria in media, and the relations between them are shown in Fig. 1. The reaction–diffusion PDE model for the stoichiometric organic matter decomposition by extending the kinetic equations in [4] to the setting of an unstirred media can be written as follows:

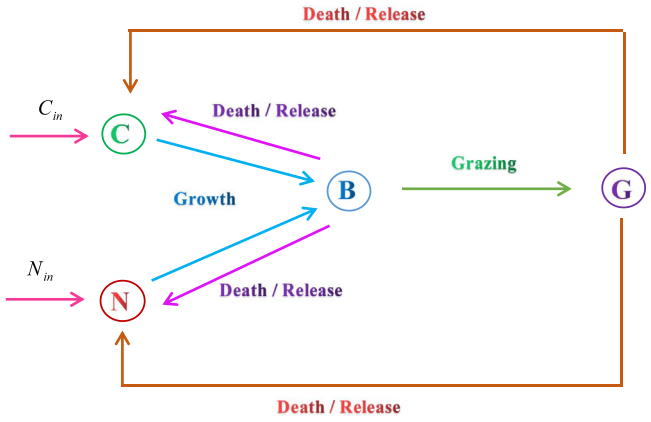

Fig. 1. A schematic diagram of relationship among variables in the model.

$$\begin{cases} B_t = d_B B_{xx} + \mu_B \Phi(N,C)B - \mu_G h(B)G - \epsilon B, & 0 < x < L,\ t > 0, \\ C_t = d_C C_{xx} - \dfrac{1}{r}\mu_B \Phi(N,C)B + \beta G + \epsilon B, & 0 < x < L,\ t > 0, \\ N_t = d_N N_{xx} + \theta_G \beta G + \theta_B \epsilon B + (\theta_B - \theta_G \alpha)\mu_G h(B)G \\ \qquad - \theta_B \mu_B \Phi(N,C)B, & 0 < x < L,\ t > 0, \\ G_t = d_G G_{xx} + \alpha \mu_G h(B)G - \beta G, & 0 < x < L,\ t > 0. \end{cases} \tag{1}$$

The boundary conditions of system (1) are

$$\begin{aligned} &W_x(0,t) = 0, \quad W_x(L,t) + qW(L,t) = 0, \qquad W = B, G, \\ &C_x(0,t) = -qC_{in}, \quad C_x(L,t) + qC(L,t) = 0, \\ &N_x(0,t) = -qN_{in}, \quad N_x(L,t) + qN(L,t) = 0, \end{aligned} \tag{2}$$

for $t > 0$ and the initial conditions are

$$\vartheta(x,0) = \vartheta^0(x), \quad \vartheta = B, C, N, G, \quad 0 < x < L. \tag{3}$$

Here we assume that the decomposition occurs in a one-dimensional space for simplicity, and we assume that bacteria, carbon, nitrogen and grazers follow passive diffusion at diffusion coefficients d_B, d_C, d_N, d_G, respectively. The growth of bacteria is governed by $\mu_B \Phi(N,C)B$, where μ_B is the maximum growth rate of bacteria, the gross bacterial growth rate is

$$\Phi(N,C) = f(N)g(C), \tag{4}$$

and $f(N)$ and $g(C)$ are the specific bacterial growth rates as functions of N or C respectively in Monod form:

$$f(N) = \frac{N}{N + k_f}, \quad g(C) = \frac{C}{C + k_g}; \tag{5}$$

the grazing of bacteria by the grazer is modeled by $-\mu_G h(B)G$, where μ_G is the maximum grazing rate and

$$h(B) = \frac{B}{B + k_h} \tag{6}$$

is the per capita grazing efficiency; and the death of bacteria is termed by $-\epsilon B$. In the grazer equation, $\alpha\mu_G h(B)G$ and $-\beta G$ describe the growth and death of the grazers respectively, where α is the conversion efficiency of bacteria to grazers measured in carbon biomass. In the carbon equation, the item $\mu_B \Phi(N,C)B/r$ represents the decomposition rate of organic substances by bacteria, which is regarded as a deputy for organic matter decomposition, where r is the proportionality constant

Table 1
List of parameters with estimated values for system (1)–(3).

Parameter	Definition	Values	Unit	References
μ_B	Maximum growth rate of bacteria	0.5	1/h	[13]
μ_G	Maximum grazing rate	0.25	1/h	[13]
k_f	Nitrogen-dependent H.S.C. for bacterial growth	1.21	mg/dm	–
k_g	Carbon-dependent H.S.C. for bacterial growth	8	mg/dm	[13]
ϵ	Bacterial death rate	0.025	1/h	[13]
r	Yield constant	0.31–0.75	–	[14,15]
θ_B	N:C of bacteria	0.11–0.25	–	[16]
θ_G	N:C of grazers	$<\theta_B$	–	[17]
k_h	H.S.C. for grazing	1	mg/dm	[13]
β	Grazer's death rate	0.0075	1/h	[13]
α	Conversion efficiency of bacteria to grazers	0–1	–	[5]
d_i	Diffusion coefficient	–	dm^2/h	–
C_{in}	Concentration of inflow carbon	–	mg/dm	–
N_{in}	Concentration of inflow nitrogen	–	mg/dm	–
q	Flow rate	–	1/dm	–

of the bacterial growth rate to the decomposition rate. Dead bacteria and grazers are assumed to recycle back to the organic carbon pool instantly, which is expressed as $\beta G+\epsilon B$. We assume that the coefficients θ_B and θ_G are the fixed $N:C$ ratios in bacteria and grazers respectively following the "strict homeostasis" assumption for heterotrophs [16,18,19]. Then $\theta_G\beta G+\theta_B\epsilon B$ in the nitrogen equation is the nitrogen recycled back from dead bacteria and grazers. The term $\mu_G h(B)G$ describes the amount of bacteria (measured in carbon biomass) consumed by grazers. Then the amount of consumed nitrogen is $\theta_B\mu_G h(B)G$, the actual amount of nitrogen used by grazers is $\theta_G\alpha\mu_G h(B)G$, and their difference $\theta_B\mu_G h(B)G-\theta_G\alpha\mu_G h(B)G$ gives the exuded nitrogen back to media. The growth of bacteria $\mu_B B\Phi(N,C)$ requires the amount of nitrogen uptake $\theta_B\mu_B B\Phi(N,C)$ with more details in [4]. In the spatially heterogeneous scenario here, we originally model the nutrient inputs by the boundary influx at $x=0$: $-qC_{in}$ for carbon and $-qN_{in}$ for nitrogen, where q is the flow rate.

The parameters in system (1)–(3) are listed in Table 1. Their values and units are adapted from the ones in [4] and will be used in our numerical simulations. The abbreviation H.S.C. represents half-saturation constant in Table 1.

3. Basic mathematical properties

In this section, we show the existence, uniqueness and *a priori* estimates of solutions of system (1)–(3) by using the theory of the abstract ordinary differential equation in [20–22] and the strong maximum principle and Hopf boundary lemma [23]. In the mathematical analysis, we assume that the diffusion coefficients of bacteria, carbon, nitrogen and grazers are the same $d_B=d_C=d_N=d_G=d$ following the approach in [24], which provides the additional conservation of masses in Theorem 3.2. This assumption is necessary for most of our analytical results, though some persistence results may still hold for unequal diffusion coefficients as shown in [25] for flow reactors. Also it is known that in practical situations [26–29], d_C, d_B, d_N have the same order of magnitude, while d_G is much smaller. So our analytic results for grazer-absent system with $G\equiv 0$ represent realistic situations. Some numerical simulations of (1)–(3) with unequal diffusion coefficients are shown in Section 6.

Let $\mathbb{X}^s=C([0,L],\mathbb{R}^s_+)$ be the positive cone of the Banach space $C([0,L],\mathbb{R}^s)$ $(s\in\mathbb{N})$ with the usual supremum norm $\|\cdot\|$. Set $u_1=B, u_2=C, u_3=N, u_4=G$ and $\mathbf{u}=(u_1,u_2,u_3,u_4)$, and the initial functions in (3) satisfying $\mathbf{u}^0=(u_1^0,u_2^0,u_3^0,u_4^0)=(B^0,C^0,N^0,G^0)\in\mathbb{X}^4$. Define the nonlinear operators $f_i:\mathbb{X}^4\to C([0,L],\mathbb{R})$ $(i=1,2,3,4)$ by

$$
\begin{aligned}
f_1(\mathbf{u}) =&\mu_B\Phi(u_3,u_2)u_1-\mu_G h(u_1)u_4-\epsilon u_1,\\
f_2(\mathbf{u}) =&-\frac{1}{r}\mu_B\Phi(u_3,u_2)u_1+\beta u_4+\epsilon u_1,\\
f_3(\mathbf{u}) =&\theta_G\beta u_4+\theta_B\epsilon u_1+(\theta_B-\theta_G\alpha)\mu_G h(u_1)u_4-\theta_B\mu_B\Phi(u_3,u_2)u_1,\\
f_4(\mathbf{u}) =&\alpha\mu_G h(u_1)u_4-\beta u_4.
\end{aligned}
$$

Consider the linear system with homogeneous boundary conditions

$$
\begin{cases}
v_t=dv_{xx}, & 0<x<L,\ t>0,\\
v_x(0,t)=0,\ v_x(L,t)+qv(L,t)=0, & t>0,\\
v(x,0)=v^0(x), & 0<x<L,
\end{cases}
\tag{7}
$$

and the linear system with non-homogeneous boundary conditions

$$
\begin{cases}
v_t=dv_{xx}, & 0<x<L, 0\le s<t,\\
v_x(0,t)=-qW_{in},\ v_x(L,t)+qv(L,t)=0, & 0\le s<t,\ W=B,G,\\
v(x,s)=v^0(x), & 0<x<L.
\end{cases}
\tag{8}
$$

By the semigroup theory presented in [21,30,31], there exists a semigroup $\mathbf{T}(t)$ on $C([0,L],\mathbb{R})$, which is positive, nonexpansive and analytic, such that

$$v(x,t)=\mathbf{T}(t)v^0(x),\quad t>0,\ 0<x<L$$

is a classical solution of system (7), and a family of affine operators $U_W(t,s)$ $(0\le s<t)$ on $C([0,L],\mathbb{R})$, such that

$$v(x,t)=U_W(t,s)v^0(x),\quad 0\le s<t,\ 0<x<L,\ W=B,G$$

is a solution of system (8). Clearly, it is true that $U_W(t,s)C([0,L],\mathbb{R}_+)\subset C([0,L],\mathbb{R}_+)$ and $\mathbf{T}(t)C([0,L],\mathbb{R}_+)\subset C([0,L],\mathbb{R}_+)$ for $0\le s<t$ and $W=B,G$. Thus, system (1)–(3) can be rewritten as

$$
\begin{aligned}
u_1(t)&=U_B(0,t)u_1^0+\int_0^t\mathbf{T}(t-\tau)f_1(\mathbf{u}(\tau))\mathrm{d}\tau,\\
u_i(t)&=\mathbf{T}(t)u_i^0+\int_0^t\mathbf{T}(t-\tau)f_i(\mathbf{u}(\tau))\mathrm{d}\tau,\ i=2,3,\\
u_4(t)&=U_G(0,t)u_2^0+\int_0^t\mathbf{T}(t-\tau)f_4(\mathbf{u}(\tau))\mathrm{d}\tau.
\end{aligned}
$$

And by the fact that $\Phi(0,u_2)=\Phi(u_3,0)=0$, $f_i(\mathbf{u})$ is quasipositive, which implies the following conclusion is true by applying Theorem 1 and Remark 1.1 in [21]:

Theorem 3.1. *Assume that the initial value function $\mathbf{u}^0\in\mathbb{X}^4$. Then system (1)–(3) has a unique mild solution $\mathbf{u}(x,t,\mathbf{u}^0)$ on $(0,\tau_{\mathbf{u}^0})$ with $\mathbf{u}(x,t,\mathbf{u}^0)=\mathbf{u}^0$ and $0<\tau_{\mathbf{u}^0}\le\infty$. Moreover, $\mathbf{u}(\cdot,t,\mathbf{u}^0)\in\mathbb{X}^4$ and $\mathbf{u}(x,t,\mathbf{u}^0)$ is a classical solution of system (1)–(3) for all $t\in(0,\tau_{\mathbf{u}^0})$.*

Furthermore, we have the following global existence, positivity and the ultimate boundedness of solutions of system (1)–(3).

Theorem 3.2. *Assume $0<r,\alpha\le 1$ and the initial value function $\mathbf{u}^0\in\mathbb{X}^4$. Then the solutions of system (1)–(3) are ultimately bounded, positive and exist globally for $t\in(0,\infty)$. That is, for any constant $0<\delta\ll 1$, there exists a $T_0>0$, such that for any $x\in[0,L]$ and $t\ge T_0$,*

$$0<W(x,t)\le\tilde{W}(x)+\delta,\qquad W=B,C,N,G,\tag{9}$$

where

$$\tilde{C}(x) = C_{in}(1+qL-qx), \quad \tilde{N}(x) = N_{in}(1+qL-qx),$$
$$\tilde{B}(x) = \min\left\{\frac{\tilde{N}(x)}{\theta_B}, \tilde{C}(x)\right\}, \quad \tilde{G}(x) = \min\left\{\frac{\tilde{N}(x)}{\theta_G}, \tilde{C}(x)\right\}. \tag{10}$$

To analyze the stability of the steady state solution, we recall the basic properties of the eigenvalue problem

$$\begin{cases} d\phi'' + p(x)\phi = \lambda\phi, & 0 < x < L, \\ \phi'(0) = 0, \quad \phi'(L) + q\phi(L) = 0, \end{cases} \tag{11}$$

and have the following well-known result: (e.g. [32, Proposition 3.1])

Lemma 3.3. *Assume $p \in \mathcal{L}^\infty([0,L])$, d and q are positive constants. Then*

(i) *The eigenvalue problem (11) has a sequence of real-valued eigenvalues satisfying*

$$\lambda_0(p) > \lambda_1(p) \geq \lambda_2(p) \geq \cdots \geq \lambda_n(p) \to -\infty,$$

as $n \to \infty$, and the corresponding eigenfunction $\phi_0(p)$ of the principal eigenvalue $\lambda_0(p)$ is positive, whereas $\phi_n(p)$ is sign-changing for each $n \in \mathbb{N}$, and

$$\lambda_0(p) = -\inf_{\phi \in H^1([0,L])/\{0\}} \frac{dq\phi^2(L) + d\int_0^L (\phi'(x))^2 dx - \int_0^L p(x)\phi^2(x)dx}{\int_0^L \phi^2(x)dx}. \tag{12}$$

(ii) *$\lambda_0(p) = \lambda_0(p,d,q)$ is continuously differentiable in p, d, q, and $\lambda_0(p_1) \geq \lambda_0(p_2)$ provided $p_1(x) \geq p_2(x)$ for $x \in [0,L]$.*

(iii) *If $p(x) \leq 0$ for each $x \in [0,L]$, then $\lambda_0(p) < 0$.*

(iv) *If $p(x) = p_1(x) + p_2$, where p_2 is a constant, then $\lambda_0(p) = \lambda_0(p_1) + p_2$. If $p(x) = p$ is a constant, then $\lambda_0(p) = p + \lambda_0(0)$, where $\lambda_0(0) = -d\omega_1^2$ and $\omega_1 \in (0, \pi/(2L))$ is the smallest positive root of $\tan(\omega L) = q/\omega$.*

4. Asymptotic analysis of the grazer–absent system

In this section, we consider the dynamics of system (1)–(3) with $G \equiv 0$, that is

$$\begin{cases} B_t = dB_{xx} + \mu_B\Phi(N,C)B - \epsilon B, & 0 < x < L,\ t > 0, \\ C_t = dC_{xx} - \frac{1}{r}\mu_B\Phi(N,C)B + \epsilon B, & 0 < x < L,\ t > 0, \\ N_t = dN_{xx} + \theta_B\epsilon B - \theta_B\mu_B\Phi(N,C)B, & 0 < x < L,\ t > 0, \\ B_x(0,t) = 0, \quad B_x(L,t) + qB(L,t) = 0, & t > 0, \\ C_x(0,t) = -qC_{in}, \quad C_x(L,t) + qC(L,t) = 0, & t > 0, \\ N_x(0,t) = -qN_{in}, \quad N_x(L,t) + qN(L,t) = 0, & t > 0, \\ \vartheta(x,0) = \vartheta^0(x), \quad \vartheta = B, C, N, & 0 < x < L. \end{cases} \tag{13}$$

From the proof of Theorem 3.2, it is known that $P = \theta_B B + N$ converges to $\tilde{N}(x)$ as $t \to \infty$. Hence, from a standard argument stated in [24], the dynamics of grazer–absent system (13) are equivalent to those of the limiting system:

$$\begin{cases} B_t = dB_{xx} + \mu_B\Phi(\tilde{N}(x) - \theta_B B, C)B - \epsilon B, & 0 < x < L,\ t > 0, \\ C_t = dC_{xx} - \frac{1}{r}\mu_B\Phi(\tilde{N}(x) - \theta_B B, C)B + \epsilon B, & 0 < x < L,\ t > 0, \\ B_x(0,t) = 0, \quad B_x(L,t) + qB(L,t) = 0, & t > 0, \\ C_x(0,t) = -qC_{in}, \quad C_x(L,t) + qC(L,t) = 0, & t > 0, \\ B(x,0) = B^0(x), \quad C(x,0) = C^0(x), & 0 < x < L. \end{cases} \tag{14}$$

Hence, we only need to study the dynamics of the limiting system (14).

Assume $B(x,t) \equiv 0$ in the limiting system (14). Then $C(x,t)$ satisfies a diffusion equation which has a unique steady state solution $C(x) = \tilde{C}(x)$. That is, $(0, \tilde{C}(x))$ is the unique trivial steady state solution of the limiting system (14), and $(0, \tilde{C}(x), \tilde{N}(x))$ is the unique trivial steady state solution of the grazer-absent system (13). The local stability of the trivial state $(0, \tilde{C}(x))$ is stated as follows.

Proposition 4.1. *For the limiting system (14), the following statements hold.*

(i) *If*

$$(H_1) \qquad \lambda_0(\mu_B\Phi(\tilde{N}(x), \tilde{C}(x))) - \epsilon < 0 \tag{15}$$

is satisfied, then the trivial steady state solution $(0, \tilde{C}(x))$ is locally asymptotically stable with respect to (14).

(ii) *If*

$$(H_2) \qquad \lambda_0(\mu_B\Phi(\tilde{N}(x), \tilde{C}(x))) - \epsilon > 0, \tag{16}$$

then $(0, \tilde{C}(x))$ is unstable with respect to (14).

We remark that the principal eigenvalue $\lambda_0(\mu_B\Phi(\tilde{N}(x), \tilde{C}(x)))$ in (H_1) or (H_2) can be estimated by

$$-d\omega_1^2 + \mu_B\Phi_{min} \leq \lambda_0(\mu_B\Phi(\tilde{N}, \tilde{C})) \leq -d\omega_1^2 + \mu_B\Phi_{max}, \tag{17}$$

where

$$\Phi_{min} := \Phi(N_{in}, C_{in}) \leq \Phi(\tilde{N}, \tilde{C}) \leq \Phi(N_{in}(1+qL), C_{in}(1+qL)) := \Phi_{max}$$

from Theorem 3.2 that $N_{in} \leq \tilde{N} \leq N_{in}(1+qL)$, $C_{in} \leq \tilde{C} \leq C_{in}(1+qL)$, and $-d\omega_1^2$ is defined in (iv) of Lemma 3.3. Moreover if $\lambda_0(\mu_B\Phi(\tilde{N}(x), \tilde{C}(x))) > 0$, then $\epsilon^* := \lambda_0(\mu_B\Phi(\tilde{N}(x), \tilde{C}(x)))$ is a critical bacterial death rate at which the stability of the trivial steady state $(0, \tilde{C}(x))$ changes. But if $\lambda_0(\mu_B\Phi(\tilde{N}(x), \tilde{C}(x))) < 0$, then (H_1) holds and $(0, \tilde{C}(x))$ is always locally asymptotically stable.

Next we show that the local stability of the trivial steady state $(0, \tilde{C}(x))$ is indeed of global nature under the same condition.

Theorem 4.2. *Assume (H_1) holds and $0 < r \leq 1$.*

(i) *If $(B(x,t), C(x,t))$ is a solution of the limiting system (14). Then*

$$\lim_{t\to\infty} B(x,t) = 0, \quad \lim_{t\to\infty} C(x,t) = \tilde{C}(x),$$

uniformly for $x \in [0,L]$.

(ii) *If $(B(x,t), C(x,t), N(x,t))$ is a solution of the grazer-absent system (13), then*

$$\lim_{t\to\infty} B(x,t) = 0, \quad \lim_{t\to\infty} C(x,t) = \tilde{C}(x), \quad \lim_{t\to\infty} N(x,t) = \tilde{N}(x)$$

uniformly for $x \in [0,L]$.

On the other hand, under the condition (H_2) (the trivial state is unstable), the system (14) is uniformly persistent so the bacteria population stays positive. We first introduce some notations as follows:

(a) $\Psi_t : \mathbb{X}^2 \to \mathbb{X}^2$ is the solution semiflow generated by the limiting system (14), where $\mathbb{X}^2$ is defined in Section 3;

(b) $\mathbb{X}_0^2 = \{(B^0, C^0) \in \mathbb{X}^2 : B(x) \not\equiv 0, \ 0 \leq x \leq L\}$, $\partial\mathbb{X}_0^2 = \mathbb{X}^2 \setminus \mathbb{X}_0^2$;

(c) $N_\partial = \{\theta^0 \in \partial\mathbb{X}_0^2 : \Psi_t(\theta^0) \in \partial\mathbb{X}_0^2, \ t \geq 0\}$;

(d) $\omega(\theta^0)$ is the omega limit set of the forward orbit $\gamma^+(\theta^0) = \{\Psi_t(\theta^0)\}_{t\geq 0}$.

The persistence under the condition (H_2) is as follows.

Theorem 4.3. *Suppose $0 < r \leq 1$ and the assumption (H_2) holds, then the limiting system (14) has a global attractor A_0 and is uniformly persistent with respect to $(\mathbb{X}_0^2, \partial\mathbb{X}_0^2)$, that is, there exists a constant $\varpi > 0$ such that $\liminf_{t\to\infty} B(\cdot, t, \theta^0) \geq \varpi$ for any $\theta^0 \in \mathbb{X}_0^2$.*

Next we discuss the existence of positive steady state solutions of the limiting system (14) bifurcating from $(0, \tilde{C}(x))$ at $\epsilon = \epsilon^* = \lambda_0(\mu_B\Phi(\tilde{N}(x), \tilde{C}(x))) > 0$. The steady state solution of the limiting system (14) satisfies

$$\begin{cases} dB'' + \mu_B\Phi(\tilde{N}(x) - \theta_B B, C)B - \epsilon B = 0, & 0 < x < L, \\ dC'' - \frac{1}{r}\mu_B\Phi(\tilde{N}(x) - \theta_B B, C)B + \epsilon B = 0, & 0 < x < L, \\ B'(0) = 0, \quad B'(L) + qB(L) = 0, \\ C'(0) = -qC_{in}, \quad C'(L) + qC(L) = 0. \end{cases} \tag{18}$$

Denote

$$\mathbb{X}_B = \{B \in H^2([0,L]) : \ B'(0)=0, \quad B'(L)+qB(L)=0\},$$
$$\mathbb{X}_C = \{C \in H^2([0,L]) : \ C'(L)+qC(L)=0\}, \quad \mathbb{Y} = \mathcal{L}^2([0,L]).$$

Define $\mathcal{F} : \mathbb{R}_+ \times \mathbb{X}_B \times \mathbb{X}_C \to \mathbb{Y}\times\mathbb{Y}\times\mathbb{R}$ as

$$\mathcal{F}(\epsilon, B(x), C(x)) = \begin{pmatrix} dB''(x) + \mu_B \Phi(\tilde{N}(x) - \theta_B B(x), C(x))B(x) - \epsilon B(x) \\ dC''(x) - \frac{1}{r}\mu_B \Phi(\tilde{N}(x) - \theta_B B(x), C(x))B(x) + \epsilon B(x) \\ C'(0) + qC_{in} \end{pmatrix}.$$

Clearly, $\mathcal{F}(\epsilon, 0, \tilde{C}(x)) = 0$ for each $\epsilon \in \mathbb{R}_+$. For $(\phi_1, \phi_2) \in \mathbb{X}_B \times \mathbb{X}_C$,

$$\mathcal{F}_{(B,C)}(\epsilon^*, 0, \tilde{C}(x)) \begin{pmatrix} \phi_1(x) \\ \phi_2(x) \end{pmatrix} = \begin{pmatrix} d\phi_1''(x) + \mu_B \Phi(\tilde{N}(x), \tilde{C}(x))\phi_1(x) - \epsilon^* \phi_1(x) \\ d\phi_2''(x) - \frac{1}{r}\mu_B \Phi(\tilde{N}(x), \tilde{C}(x))\phi_1(x) + \epsilon^* \phi_1(x) \\ \phi_2'(0) \end{pmatrix}.$$

We have the following existence of positive solutions of (18) via bifurcation theory.

Theorem 4.4. *Assume that $0 < r \le 1$ and $\epsilon^* := \lambda_0(\mu_B \Phi(\tilde{N}(x), \tilde{C}(x))) > 0$. Then*

(i) *there exists a positive constant $\sigma \ll 1$, such that positive solutions $(\epsilon(s), B(s,x), C(s,x))$ $(s \in (0,\sigma), x \in [0,L])$ of system (18) bifurcating from $(0, \tilde{C}(x))$ at $\epsilon = \epsilon^*$, and they lie on a smooth curve*

$$\Gamma_1^+ = \{(\epsilon(s), B(s,x), C(s,x)) : \ s \in (0,\sigma), \quad x \in [0,L]\}$$

satisfying $B(s,x) = s\eta_0(x) + sw_1(s,x)$, $C(s,x) = \tilde{C}(x) + s\zeta_0(x) + sw_2(s,x)$, $\epsilon(0) = \epsilon^*$, and $w_i(0,x) = 0$ for $i = 1,2$, where $\eta_0(x) > 0$ is the principal eigenfunction of (11) with $p(x) = \mu_B \Phi(\tilde{N}(x), \tilde{C}(x))$, and

$$\zeta_0(x) := (-d\Delta)^{-1}\left(\epsilon^* - \frac{\mu_B}{r}\Phi(\tilde{N}(x), \tilde{C}(x))\right)\eta_0(x) < 0. \tag{19}$$

(ii) *The bifurcation at $\epsilon = \epsilon^*$ satisfies $\epsilon'(0) < 0$ so $\epsilon(s) < \epsilon^*$ for $s \in (0,\sigma)$ and bifurcating positive solutions exist for $\epsilon \in (\epsilon^* - \sigma, \epsilon^*)$ for some $\sigma > 0$, and the bifurcating positive solution $(\epsilon(s), B(s,x), C(s,x))$ is locally asymptotically stable with respect to the limiting system (14) for $s \in (0,\sigma)$.*

Now we show that the local bifurcation of positive solutions of (18) is of global nature, and the positive solutions exist for all $\epsilon \in (0, \epsilon^*)$. Let the set of nontrivial solutions of (18) be

$$\Xi := \{(\epsilon, B, C) \in (0,\infty) \times \mathbb{X}_B \times \mathbb{X}_C : \ \mathcal{F}(\epsilon, B(x), C(x)) = 0, \ (B(x), C(x)) \neq (0, \tilde{C}(x))\}.$$

Also in Theorem 4.4, the branch of nontrivial solutions of (18) can be decomposed into the following two parts:

$$\Gamma_1^+ = \{(\epsilon(s), B(s,x), C(s,x)) : \ s \in (0,\sigma), \ x \in [0,L]\},$$
$$\Gamma_1^- = \{(\epsilon(s), B(s,x), C(s,x)) : \ s \in (-\sigma, 0), \ x \in [0,L]\}.$$

Then the global bifurcation of positive solutions of (18) is described below. It is similar to the ones in [33–35].

Theorem 4.5. *Assume that $0 < r \le 1$ and $\epsilon^* := \lambda_0(\mu_B \Phi(\tilde{N}(x), \tilde{C}(x))) > 0$. Then there exists a connected component $\mathcal{C}$ of the closure of Ξ such that the curve Γ_1 obtained in Theorem 4.4 is contained in $\mathcal{C}$. Moreover let $\mathcal{C}^+$ be the connected component of $\mathcal{C}/\Gamma_1^-$ containing Γ_1^+, then all solutions of (18) on $\mathcal{C}^+$ are positive, and the projection of $\mathcal{C}^+$ onto ϵ-axis $\mathrm{Proj}_\epsilon \mathcal{C}^+ = (0, \epsilon^*)$.*

Summarizing the results in Theorems 4.2, 4.3, 4.4 and 4.5, we have the following complete classification of dynamical behaviors of the grazer–absent system:

Corollary 4.6. *Assume that $0 < r \le 1$ and $\epsilon^* := \lambda_0(\mu_B \Phi(\tilde{N}(x), \tilde{C}(x))) > 0$.*

(i) *When $\epsilon > \epsilon^*$ (or equivalently (H_1) holds), the grazer–absent system (13) has no positive steady state solution, and the trivial steady state $(B, \tilde{C}(x), \tilde{N}(x))$ is globally asymptotically stable.*

(ii) *When $0 < \epsilon < \epsilon^*$ (or equivalently (H_2) holds), the grazer–absent system (13) is uniformly persistent and there exists at least one positive steady state solution $(B_1(x), C_1(x), N_1(x))$ with $N_1(x) = \tilde{N}(x) - \theta_B B_1(x)$ and $B_1(x) > 0$. Moreover the positive steady state is unique and is locally asymptotically stable for $\epsilon \in (\epsilon^* - \sigma, \epsilon^*)$ for some $\sigma > 0$.*

5. Asymptotic analysis of the grazer–present system

In this section, we discuss the dynamics of the grazer–present system (1)–(3). By Theorem 3.2 and substituting $\tilde{N}(x) - \theta_B B(x,t) - \theta_G G(x,t)$ for $N(x,t)$ in the system, we obtain the following limiting system with equivalent asymptotic dynamics:

$$\begin{cases} B_t = dB_{xx} + \mu_B \Phi(\tilde{N}(x) - \theta_B B - \theta_G G, C)B \\ \qquad - \mu_G h(B)G - \epsilon B, & 0 < x < L, t > 0, \\ C_t = dC_{xx} - \frac{1}{r}\mu_B \Phi(\tilde{N}(x) - \theta_B B - \theta_G G, C)B \\ \qquad + \beta G + \epsilon B, & 0 < x < L, \ t > 0, \\ G_t = dG_{xx} + \alpha\mu_G h(B)G - \beta G, & 0 < x < L, \ t > 0, \\ B_x(0,t) = 0, \quad B_x(L,t) + qB(L,t) = 0, & t > 0, \\ C_x(0,t) = -qC_{in}, \quad C_x(L,t) + qC(L,t) = 0, & t > 0, \\ G_x(0,t) = 0, \quad G_x(L,t) + qG(L,t) = 0, & t > 0, \\ B(x,0) = B^0(x), \quad C(x,0) = C^0(x), \quad G(x,0) = G^0(x), & 0 < x < L. \end{cases} \tag{20}$$

From Section 4, the limiting system (20) has a unique trivial steady state solution, denoted as $E_0 = (0, \tilde{C}(x), 0)$. The stability of E_0 with respect to the grazer-present limiting system (20) inherits from the one for the grazer-absent limiting system (14) for any grazer's death rate $\beta > 0$.

Theorem 5.1. *Assume $0 < r, \alpha \le 1$ and $\beta > 0$. For the limiting system (20), the following statements are true:*

(i) *If (H_1) holds, then E_0 is globally asymptotically stable;*

(ii) *If (H_2) holds, then E_0 is unstable, and there exists a semi-trivial steady state solution $E_1 = (B_1(x), C_1(x), 0)$ with $B_1(x), C_1(x) > 0$ when $0 < \epsilon < \epsilon^*$ provided $\epsilon^* > 0$. Moreover, E_1 is locally asymptotically stable when $\epsilon^* - \sigma < \epsilon < \epsilon^*$.*

Theorem 5.1 shows that when bacteria become extinct, grazers cannot survive either no matter how small the death rate is, and the system will settle at the extinction state E_0.

Next we show that when bacteria persist, how the persistence of grazers is determined by the death rate of grazers. More precisely the uniform persistence and the existence of positive steady state solutions of the limiting system (20) are established under (H_2) and additional conditions. There are three types of nonnegative steady state solutions of system (20):

(i) the trivial steady state solution $E_0 = (0, \tilde{C}(x), 0)$, which always exists;

(ii) the semi-trivial steady state solution $E_1 = (B_1(x), C_1(x), 0)$ with $B_1(x) > 0$ and $C_1(x) > 0$, which exists for $x \in [0,L]$ provided $0 < r \le 1$ and (H_2) hold;

(iii) the coexistent steady state solution $E_2 = (B_2(x), C_2(x), G_2(x))$ with $B_2(x) > 0$, $C_2(x) > 0$ and $G_2(x) > 0$ for all $x \in [0,L]$.

To observe that E_0, E_1 and E_2 are all possible forms of nonnegative steady state solutions of (20), let $(B(x), C(x), G(x))$ be a nonnegative steady state solution of system (20) which is not E_2. From the strong

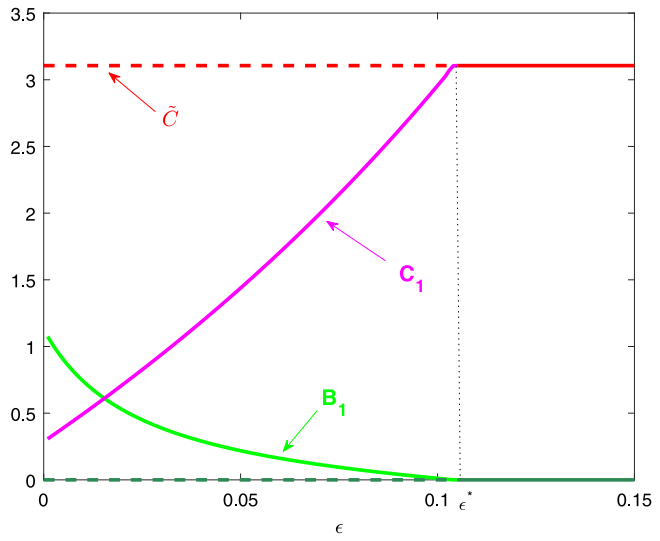

Fig. 2. The bifurcation diagram of the limiting grazer-absent system (14) with the bifurcation parameter ϵ showing the transcritical bifurcation. Other parameter values are given in P_0. The horizontal axis is $\epsilon \in (0, 0.15)$, and the vertical axis is the total biomass. The solid curves represent stable solutions and the dotted curves represent unstable solutions.

maximum principle, each component is either zero or strictly positive. If $B(x) \equiv 0$, then $G(x)$ satisfies

$$\begin{cases} dG'' - \beta G = 0, \quad 0 < x < L, \\ G'(0) = 0, \quad G'(L) + qG(L) = 0, \end{cases}$$

which implies that $G(x) \equiv 0$, and the solution must be E_0. On the other hand, if $B(x) > 0$ and $G(x) > 0$ for $x \in [0, L]$, one has E_2 form, which is a coexistence state; and if $B(x) > 0$ and $G(x) \equiv 0$ for $x \in [0, L]$, one has E_1 form. Consequently, E_0, E_1 and E_2 are all possible forms of nonnegative steady state solutions of (20). We have shown that E_0 is unique, and E_1 exists under (H_2) but the uniqueness is unknown. We prove the existence of E_2 (a positive coexistence state) under (H_2) and additional conditions by using persistence theory.

For convenience, we first introduce some notations. Setting $\widetilde{\Psi}_t : \mathbb{X}^3 \to \mathbb{X}^3$ be the solution semiflow generated by the limiting system (20). Let

$$\begin{aligned} \mathbb{X}_1^3 &= \{(B, G, C) \in \mathbb{X}^3 : \ B(x) \not\equiv 0, \ G(x) \not\equiv 0, \ \ 0 \le x \le L\}, \\ \partial\mathbb{X}_1^3 &= \mathbb{X}^3 \setminus \mathbb{X}_1^3, \\ N_\partial^1 &= \{\Theta^0 \in \partial\mathbb{X}_1^3 : \ \widetilde{\Psi}_t(\Theta^0) \in \partial\mathbb{X}_1^3, \ \ t \ge 0\}, \end{aligned}$$

and let $\widetilde{\omega}(\Theta^0)$ be the omega limit set of the forward orbit $\widetilde{\gamma}^+(\Theta^0) = \{\widetilde{\Psi}_t(\Theta^0)\}_{t\ge 0}$. Let $\mathcal{P} : \mathbb{X}^2 \to C([0, 1], \mathbb{R}_+)$ be the projection on $\mathbb{X}^2$, defined by $\mathcal{P}(B, C) = B$ for $(B, C) \in \mathbb{X}^2$.

The following main theorem indicates that the existence of the coexistent steady state listed in (iii) and the proof is given in the Appendix.

Theorem 5.2. *Assume that and $0 < r, \alpha \le 1$, (H_2) holds, and let A_0 be the global attractor of limiting grazer–absent system (14). In addition, assume that*

$$(H_3) \qquad \lambda_0\left(\alpha\mu_G \inf_{B\in\mathcal{P}(A_0)} h(B(x))\right) - \beta > 0 \tag{21}$$

holds. Then system (20) has a global attractor A_1 and is uniformly persistent with respect to $(\mathbb{X}_1^3, \partial\mathbb{X}_1^3)$, that is, there exists a constant $\varpi_1 > 0$, such that for any solution $(B(x,t), C(x,t), G(x,t))$ with the initial condition $\Theta^0 = (B^0, C^0, G^0) \in \mathbb{X}_1^3$,

$$\liminf_{t\to\infty} B(x, t, \Theta^0(x)) \ge \varpi_1, \qquad \liminf_{t\to\infty} G(x, t, \Theta^0(x)) \ge \varpi_1, \quad x \in [0, L].$$

Furthermore, system (20) admits at least one positive steady state solution E_2.

We remark that if $\lambda_0\left(\alpha\mu_G \inf_{B\in\mathcal{P}(A_0)} h(B(x))\right) < 0$, then (H_3) holds automatically for any $\beta > 0$; and if $\lambda_0\left(\alpha\mu_G \inf_{B\in\mathcal{P}(A_0)} h(B(x))\right) := \beta^* > 0$, the assumption (H_3) is equivalent to $0 < \beta < \beta^*$.

Applying Theorems 5.1 and 5.2 to the full grazer–present system (1)–(3), we obtain

Corollary 5.3. *Assume that $0 < r, \alpha \le 1$, $\epsilon^* = \lambda_0(\mu_B\Phi(\tilde{N}(x), \tilde{C}(x))) > 0$ and $\beta^* = \lambda_0\left(\alpha\mu_G \inf_{B\in\mathcal{P}(A_0)} h(B(x))\right) > 0$.*

(i) *When $\epsilon > \epsilon^*$ (or equivalently (H_1) holds) and $\beta > 0$, the grazer–present system (1)–(3) has no positive steady state solution, and the trivial steady state $(0, \tilde{C}(x), \tilde{N}(x), 0)$ is globally asymptotically stable.*

(ii) *When $0 < \epsilon < \epsilon^*$ (or equivalently (H_2) holds), the grazer–present system (1)–(3) has at least one semi-trivial steady state solution $(B_1(x), C_1(x), N_1(x), 0)$ with $N_1(x) = \tilde{N}(x) - \theta_B B_1(x)$ and $B_1(x) > 0$. Moreover the semi-trivial steady state is unique and locally asymptotically stable when $\epsilon^* - \sigma < \epsilon < \epsilon^*$ for some $\sigma > 0$.*

(iii) *When $0 < \epsilon < \epsilon^*$ (or equivalently (H_2) holds) and $0 < \beta < \beta^*$ (or equivalently (H_3) holds), the grazer–present system (1)–(3) is uniformly persistent, and there exists at least one positive steady state solution $(B_2(x), C_2(x), N_2(x), G_2(x))$ with $N_1(x) = \tilde{N}(x) - \theta_B B_2(x) - \theta_G G_2(x)$, $B_2(x) > 0$ and $G_2(x) > 0$.*

6. Numerical simulations

In this section, we use numerical simulations of the limiting grazer-absent system (14) and the limiting grazer-present system (20) to illustrate our theoretical conclusions obtained in Sections 4 and 5, and to provide some new insights on the biodegradation. In this section, the curves in figures represent the total mass of functions (L^1 norm of the functions).

The initial conditions are chosen as

$$\begin{aligned} &B^0(x) = 0.03 + 0.01\sin(\pi x), C^0(x) = 3 + 0.1\cos(\pi x), \\ &G^0(x) = 0.03 + 0.01\cos(\pi x), \end{aligned} \tag{22}$$

and other parameters are chosen as follows:

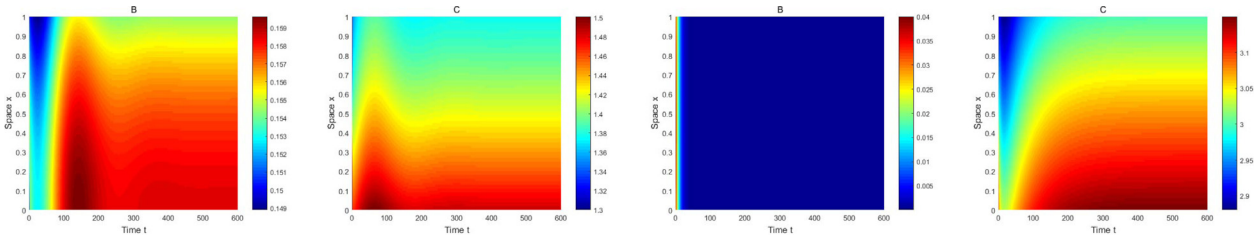

Fig. 3. The solutions of system (14) for different ϵ. Left: the solution converges to a positive steady state as $\epsilon = 0.05 < \epsilon^* = 0.105$. Right: the solution converges to $(0, \tilde{C}(x))$ as $\epsilon = 0.2 > \epsilon^* = 0.105$.

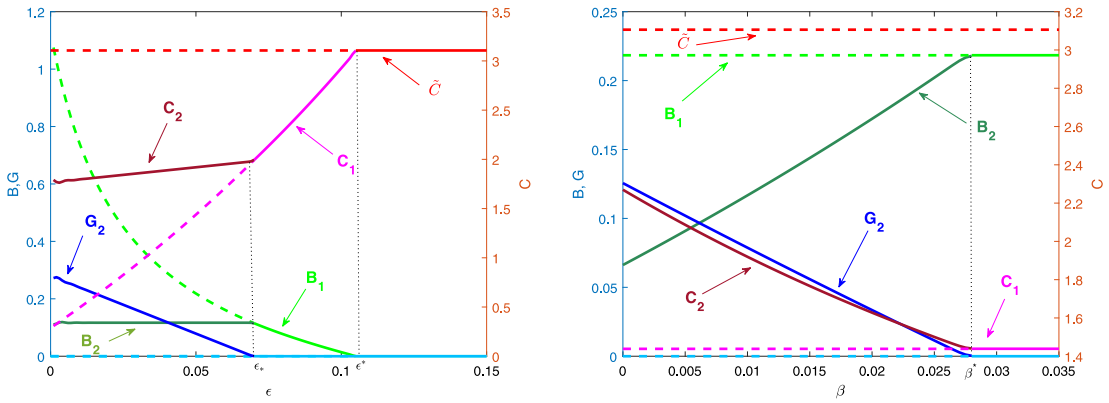

Fig. 4. The bifurcation diagrams of the limiting grazer-present system (20) showing transcritical bifurcations. Left: bifurcation parameter ϵ; Right: bifurcation parameter β and $\epsilon = 0.05$. All other parameter values are given in P_0. The horizontal axis is the bifurcation parameter, and the vertical axis is the total biomass. The solid curves represent stable solutions and the dotted curves represent unstable solutions.

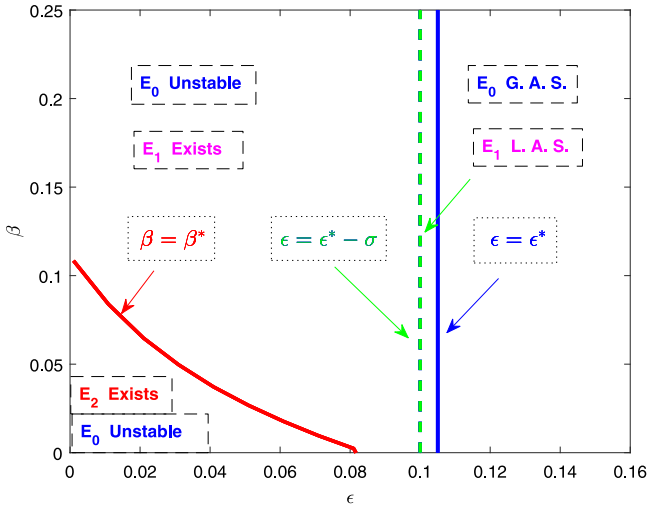

Fig. 5. The ϵ–β plane diagram for the limiting grazer–present system (20). Here $\epsilon^* = 0.105$ and $\beta^* = 0.0277$ when $\epsilon = 0.05$, and other parameter values are given in P_0. Here the abbreviation G.A.S. represents globally asymptotically stable and L.A.S. represents locally asymptotically stable.

$$P_0 : \mu_B = 0.5, k_f = 1.21, k_g = 8, k_h = 1, \theta_B = 0.25, r = 0.4, \mu_G = 0.25, \theta_G = 0.1, \alpha = 0.95, \beta = 0.01, C_{in} = 3, N_{in} = 7, q = 0.05, d = 0.3, L = 1 \text{ and } \epsilon = 0.05.$$

With these parameter values, we have $\tilde{N}(x) = 7.35 - 0.35x$, $\tilde{C}(x) = \tilde{B}(x) = \tilde{G}(x) = 3.15 - 0.15x$, $\epsilon^* = \lambda_0(\mu_B \Phi(\tilde{N}(x), \tilde{C}(x))) = 0.105$, and $\beta^* = \lambda_0 \left(\alpha \mu_G \inf_{B \in \mathcal{P}(A_0)} h(B(x))\right) = 0.0277$ when $\epsilon = 0.05$. Hence, (H_1) holds if $\epsilon > 0.105$; (H_2) holds if $\epsilon < 0.105$; and (H_3) holds if $0 < \beta < 0.027$.

Fig. 2 shows the bifurcation diagram for system (14) with the bacterial death rate ϵ as the bifurcation parameter, which verifies the conclusions of Proposition 4.1 and Theorem 4.4. Fig. 3 shows the solution trajectories of (14) before and after the bifurcation value ϵ^*. When $\epsilon < 0.105$, the solution of system (14) converges to a positive steady state, and when $\epsilon > 0.105$, the solution converges to the trivial state $(0, \tilde{C}(x))$. That is, when ϵ is large, organic carbon cannot be decomposed and bacteria become extinct, and when ϵ is small, bacteria survive and can partly decompose organic carbon.

Fig. 4 shows two bifurcation diagrams of the limiting system (20), which illustrates the conclusions in Theorems 5.1 and 5.2. When using the bacterial death rate ϵ as the bifurcation parameter, the system (20) has two thresholds, a critical bacterial death rate $\epsilon^* = 0.105$ from the condition (H_1), and $\epsilon_* = 0.07$ from (H_3) for fixed $\beta = 0.01$, while other parameters are fixed as in P_0. When $\epsilon > \epsilon^*$, all solutions converge to the trivial steady state solution E_0; when $\epsilon_* < \epsilon < \epsilon^*$, the semi-trivial steady state solution E_1 exists and it appears to be unique and asymptotically stable; and when $0 < \epsilon < \epsilon_*$, a positive steady state solution E_2 exists and attracts all solutions (see the left panel of Fig. 4). It is interesting to observe that the bacterial biomass $B_2(x)$ almost stays at the same level for all $0 < \epsilon < \epsilon_*$, but $C_2(x)$ is smaller as ϵ decreases so the presence of grazers does facilitate the decomposition of organic carbon.

On the other hand, fixing ϵ at 0.05 and using the grazer's death rate β as the bifurcation parameter, system (20) has a critical grazer's death rate $\beta^* = 0.0277$ from the condition (H_3), below which the system possesses a positive steady state E_2 (see the right panel of Fig. 4). The existence and stability parameter regimes of steady states E_0, E_1 and E_2 are shown in the $\epsilon - \beta$ bifurcation diagram in Fig. 5. The region below the curve $\beta = \beta^*$ is where a coexistence state E_2 exists. Fig. 6 shows several solution trajectories of the limiting grazer-present system (20) with different parameter values of ϵ and β. Here the solution converges to E_0 when $\epsilon = 0.2 > \epsilon^* = 0.105$ (first row); the solution converges to E_1 when $\epsilon = 0.05 < \epsilon^* = 0.105$ and $\beta = 0.04 > \beta^* = 0.0277$; and the solution converges to the positive steady state solution E_2 when $\epsilon = 0.05$ and $\beta = 0.01 < \beta^*$. It is known that [26–29], d_C, d_B, d_N have the same order of magnitude, while d_G is much smaller. In Fig. 7 we show the same effect of ϵ and β as Fig. 6 but for the full system (1) with $d_B = 0.5$, $d_C = 0.3$, $d_G = 0.005$ and $d_N = 1$ so that the mass conservation with equal diffusion coefficients no longer holds. The behaviors of the solutions in this case are similar to the ones in Fig. 6.

Fig. 8 shows the bifurcation diagram with respect to the concentration of inflow carbon C_{in} as the bifurcation parameter. There are three bifurcation values: $S_1 = 1.4$, $S_2 = 2.5$ and $S_3 = 5.5$. If $C_{in} < S_1$, then only E_0 exists and neither bacteria nor grazers can survive; if $S_1 < C_{in} < S_2$, then E_1 is the attracting state, so bacteria persist but their biomass is not sufficient to support the persistence of grazers; if $S_2 < C_{in} < S_3$, then E_2 is the attracting state, and bacteria and grazers coexist at an interior steady state; and if $C_{in} > S_3$, the coexistence steady state E_2 appears to become unstable, and a limit cycle becomes the attracting state. Thus S_3 is a Hopf bifurcation point (shown numerically). For $C_{in} > S_3$, there are two curves representing the maximum and minimum of periodic solutions in Fig. 5. This implies that an increase of the carbon input C_{in} can support bacteria, a further increase would also support grazers, and a very large carbon input causes temporal oscillations of the system. This appears to be a paradox of enrichment phenomenon. Again for the intermediate carbon input $(S_2 < C_{in} < S_3)$, the bacterial steady state biomass $B_2(x)$ is nearly same, while carbon and grazers increase in a linear fashion with respect to C_{in}.

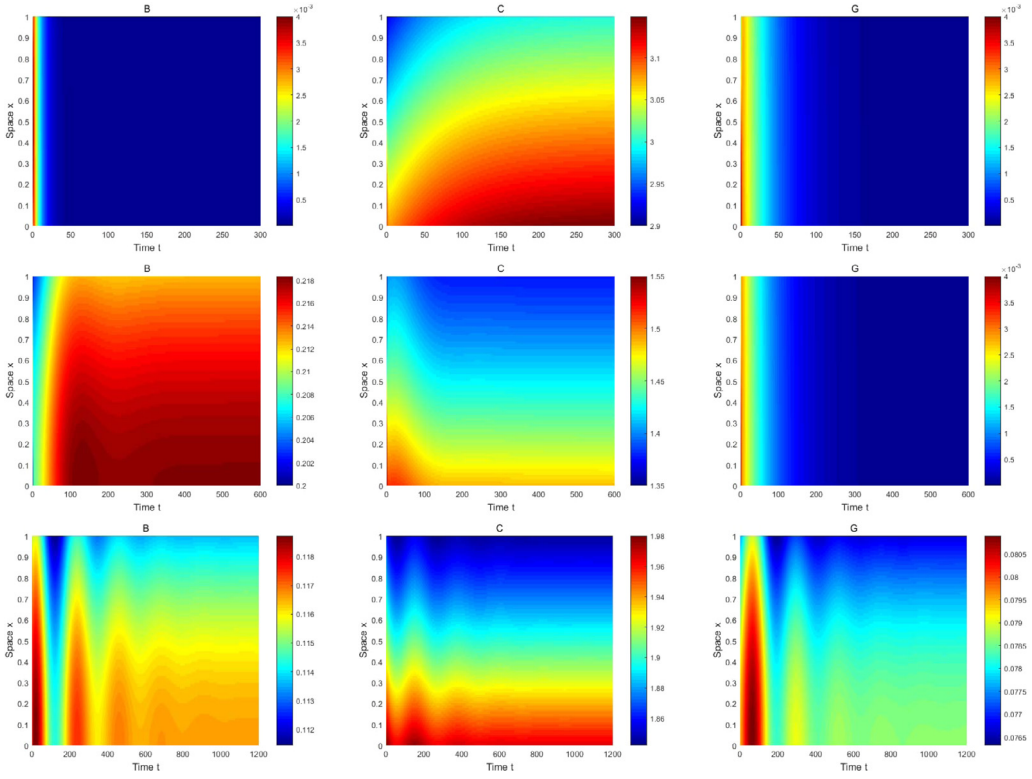

Fig. 6. Effects of parameters ϵ and β on solutions of the limiting grazer-present system (20). First row: $\epsilon = 0.2$, $\beta = 0.01$. Second row: $\epsilon = 0.05$, $\beta = 0.04$. Third row: $\epsilon = 0.05$, $\beta = 0.01$. Other parameter values are given in P_0.

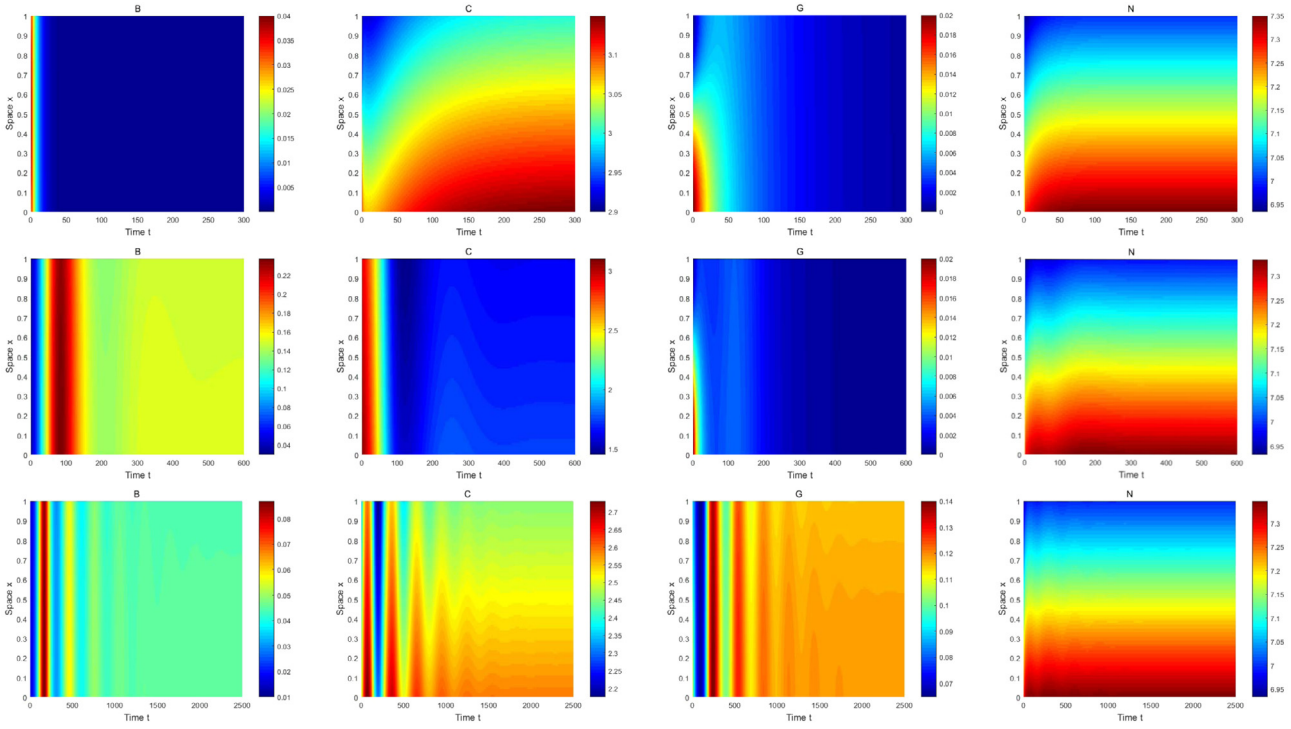

Fig. 7. Effects of parameters ϵ and β on solutions of system (1) with $d_B = 0.5$, $d_C = 0.3$, $d_G = 0.005$, $d_N = 1$. First row: $\epsilon = 0.2$, $\beta = 0.01$. Second row: $\epsilon = 0.05$, $\beta = 0.04$. Third row: $\epsilon = 0.05$, $\beta = 0.01$. Other parameter values are given in P_0.

Fig. 9 shows the solution trajectories in these four cases: when $C_{in} = 1 < S_1 = 1.4$, the solution converges to E_0 and both bacteria and grazers go extinct; when $S_1 < C_{in} = 2 < S_2 = 2.5$, the solution converges to E_1, grazers go extinct and bacteria persist; when $S_2 < C_{in} = 3 < S_3 = 5.5$, the solution converges to E_2, and both bacteria and grazers persist and settle at an interior steady state; and when $C_{in} = 6 > S_3$, the solution appears to converge to a stable limit cycle. Fig. 10 shows the effect of the parameter C_{in} on solutions of the full system (1) with different

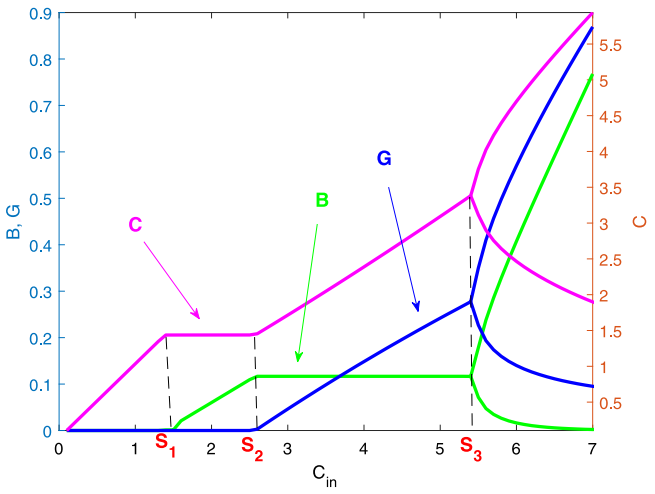

Fig. 8. Bifurcation diagram for the limiting system (20) by taking C_{in} as a bifurcating parameter and keep other parameters fixed as in P_0. For $C_{in} > S_3$, the maximum and minimum of periodic solutions are shown so the asymptotic dynamics is oscillatory.

diffusion coefficients $d_B = 0.5$, $d_C = 0.3$, $d_G = 0.005$ and $d_N = 1$ as in Fig. 7. Again the behaviors of the solutions in this case are similar to the ones in Fig. 9.

Fig. 11 shows the transient oscillatory dynamics of system (20) when ϵ is sufficiently small. As ϵ decreases, transient oscillations stay longer. Eventually the solution always converges to the interior steady state whose carbon biomass is similar for different tiny ϵ values. This observation is informative to experiments in which most researchers assume a zero bacterial death rate. Here we show how a tiny bacterial death rate regulates the transient and asymptotic dynamics.

Finally we use sensitivity analysis to examine the influence of system parameters on the decomposition rate, which represents the decomposition efficiency in the grazer-present system (1), and it can be written as

$$R^P(t) = \frac{\mu_B}{r}\int_0^L B(x,t)\Phi(\tilde{N}(x) - \theta_B B(x,t) - \theta_G G(x,t), \tilde{C}(x))dx; \tag{23}$$

and in the grazer-absent system (13), it becomes

$$R^A(t) = \frac{\mu_B}{r}\int_0^L B(x,t)\Phi(\tilde{N}(x) - \theta_B B(x,t), \tilde{C}(x))dx. \tag{24}$$

As the solution approaches a steady state as $t \to \infty$, the decomposition rate converges as well, and we can assume that $R^W = \lim_{t\to\infty} R^W(t)$ to be the steady state decomposition rate of the system for $W = P$ or A. By applying the normalized forward sensitivity index and the modified

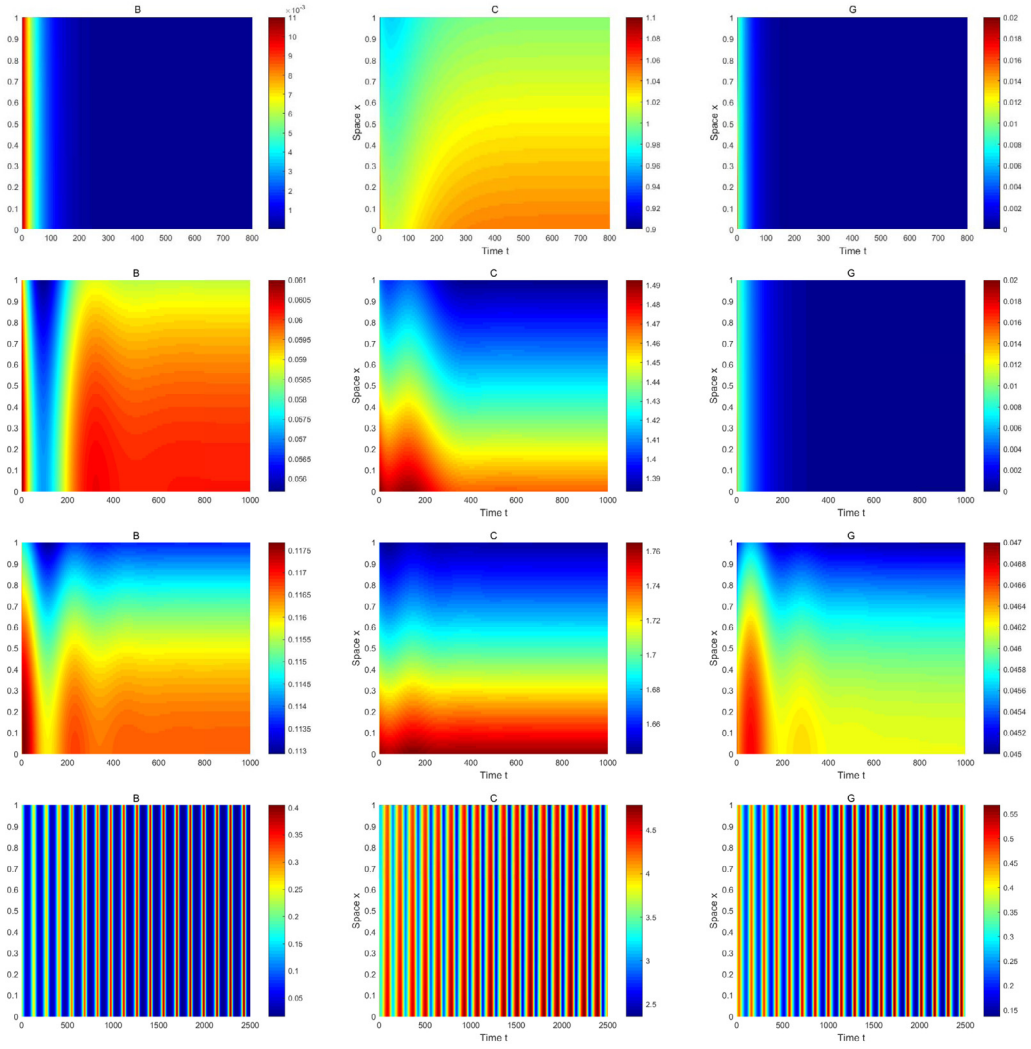

Fig. 9. The effect of parameter C_{in} on solutions of the limiting grazer-present system. First row: $C_{in} = 1$; second row: $C_{in} = 2$; third row: $C_{in} = 3$; fourth row: $C_{in} = 6$. Other parameter values are given in P_0.

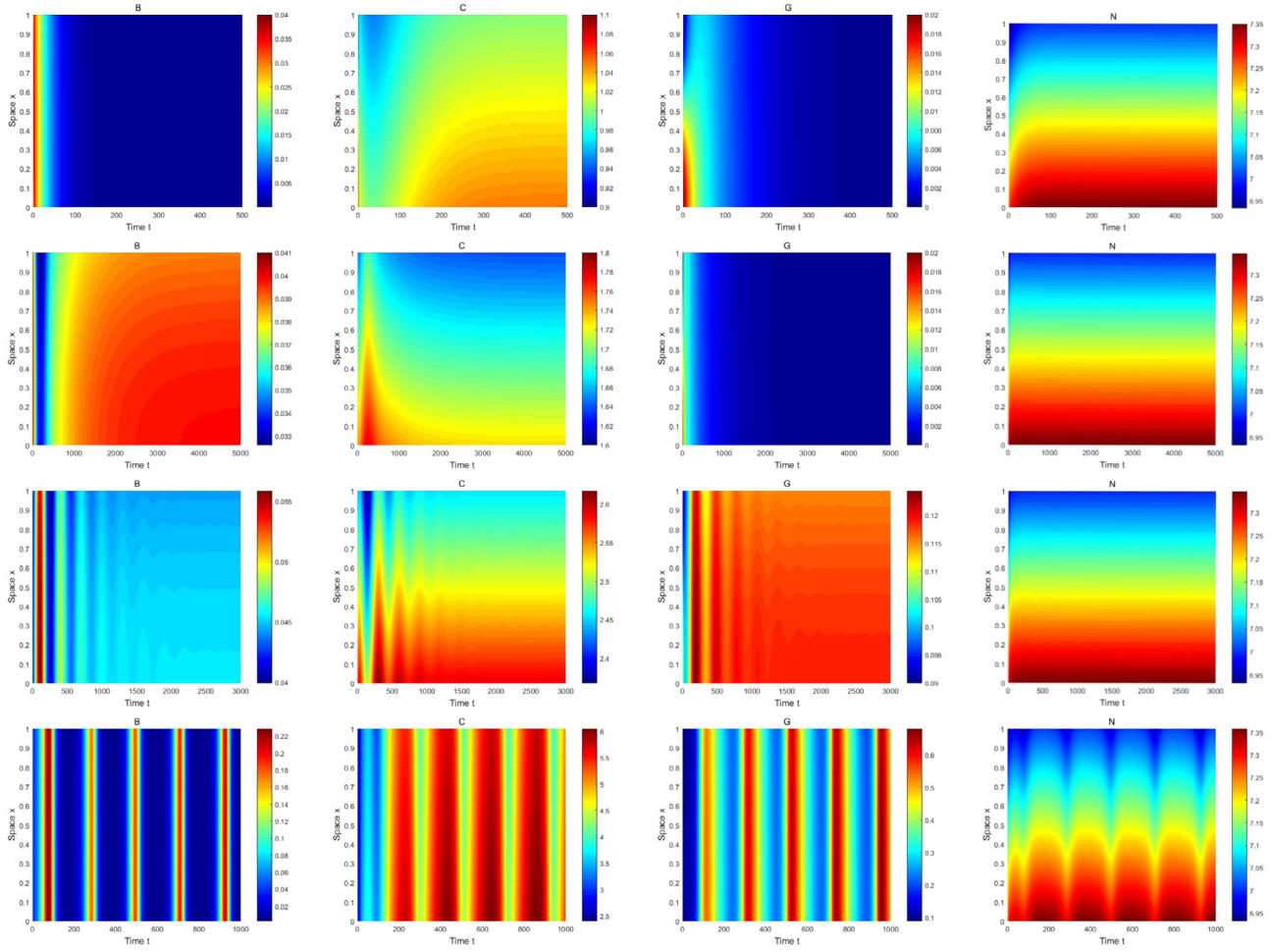

Fig. 10. The effect of parameter C_{in} on solutions of system (1) with $d_B = 0.5$, $d_C = 0.3$, $d_G = 0.005$, $d_N = 1$. First row: $C_{in} = 1$; second row: $C_{in} = 2$; third row: $C_{in} = 3$; fourth row: $C_{in} = 6$. Other parameter values are given in P_0.

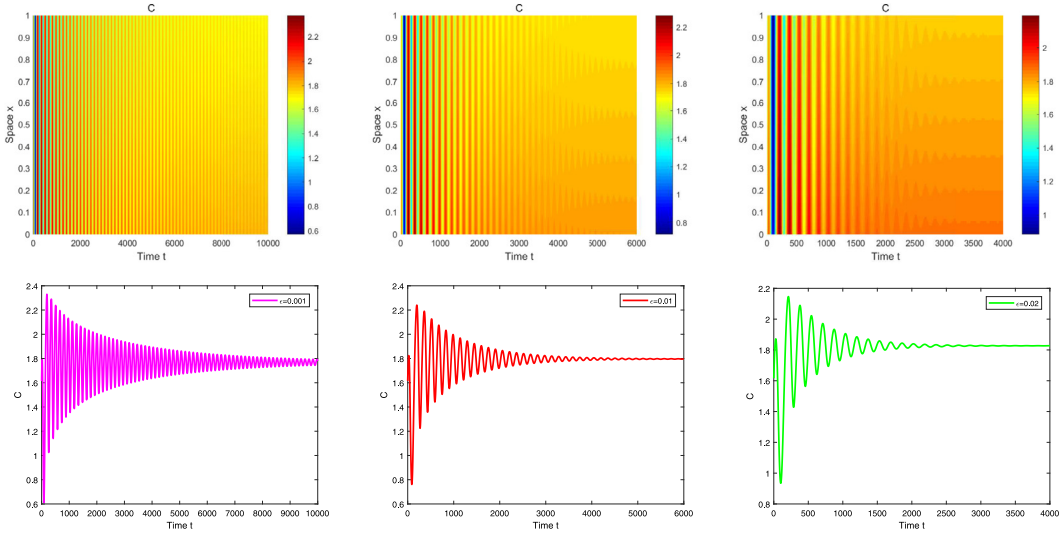

Fig. 11. The transient dynamics in system (20) with small ϵ. Here $\epsilon = 0.001, 0.01$ and 0.02 in the first, second and third columns. Other parameter values are given in P_0.

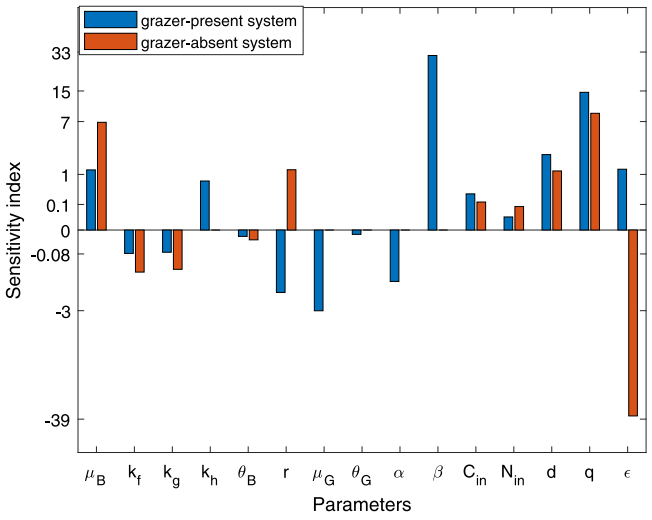

Fig. 12. The sensitivity indices of the degradation rate to the parameters. Baseline parameter values are given in P_0.

Table 2
The sensitivity indices of the degradation rate to the parameters.

Parameter	S.I. for grazer-present system	S.I. for grazer-absent system
μ_B	1.2637	7.2639
k_f	−0.0747	−0.4328
k_g	−0.0637	−0.3531
k_h	0.6849	0
θ_B	−0.0015	−0.0055
r	−1.4130	1.2728
μ_G	−3.0593	0
θ_G	-4.7007×10^{-4}	0
α	−0.7894	0
β	31.9042	0
C_{in}	0.2745	0.1275
N_{in}	0.013	0.075
d	2.4932	1.1987
q	15.1759	9.244
ϵ	1.3067	−37.3386

numerical formula obtained by the central difference approximation in [4,36], the sensitivity index can be written as

$$Y_p = \frac{R^W(1.01p) - R^W(0.99p)}{0.02R^W(p)}, \tag{25}$$

where $R^W(p)$ is the steady state decomposition rate with a parameter p, and $W = P$ or A.

We calculate the sensitivity index (SI) for each of the 15 parameters listed in Table 1 while other parameters are fixed as in P_0, using the limiting grazer–present system (20) with $\epsilon = 0.05$ (for the grazer–present system), and with $\epsilon = 0.08$ (for the grazer–absent system as the solution converges to E_1). The results are shown in Table 2 and Fig. 12. In the grazer–present system, the decomposition rate is most sensitive to the grazer's death rate, while in the grazer-absent system, the decomposition rate is most sensitive to the bacterial death rate. Therefore, we choose these two death rates as the primary parameters in most of our mathematical results.

When the sensitivity index in Table 2 is positive, the corresponding parameter has a positive effect on the decomposition rate. In the grazer–present system, increasing the flow rate q can increase the decomposition rate, and the grazer's death rate β also has a great positive effect on the decomposition rate. In the grazer–absent system, the relationships are similar to those found in [4]. Again increasing the flow rate q can accelerate the decomposition. On the other hand, the bacterial death rate ϵ has a great negative effect on the decomposition rate.

In Figs. 13–15, we examine the dependence of the decomposition rates in the grazer–absent/–present systems on key parameters over their wide ranges with all other parameters (except the bifurcation parameter) fixed as in P_0. Fig. 13 shows that as one of the parameters d, ϵ, μ_B and q increases, the decomposition rates R^A and R^P corresponding to the grazer-absent/-present systems both increase. Large d, ϵ or q, or small μ_B inhibits the grazer's facilitation effect on biodegradation. On the other hand, when one of the parameters k_f, k_g, θ_B and r increases, the decomposition rate R^P corresponding to the grazer–present system decreases, as shown in Fig. 14. However, the decomposition rate R^A corresponding to the grazer-absent system only decreases as r increases, and almost irrelevant to the parameters k_f, k_g, θ_B. Furthermore, large k_f, k_g or θ_B inhibits the grazer's facilitation effect on biodegradation, while r almost has no impact on the facilitation effect. The influences of the parameters C_{in} and N_{in} on the decomposition rates are not monotone, as shown in Fig. 15. There is an optimal nitrogen input concentration for making the organic matter decomposition most efficient in the absence or presence of grazing. Note that oscillations in C_{in} graph are caused by the emergence of limit cycles in large C_{in} regime. Small C_{in} or N_{in} inhibits the grazer's facilitation effect on biodegradation.

A common feature in Figs. 13–15 is that the decomposition rate for the grazer-present system R^P is greater than or equal to the one for the grazer-absent system R^A, which indicates that the decomposition rate increases if bacterivorous grazers are added to the decomposition process. This resolves the "decomposition–facilitation paradox" [5–10,37] in the spatial PDE context.

7. Discussion

In this paper, we explore the dynamical behaviors of a stoichiometric bacteria–grazer reaction–diffusion model for organic matter decomposition. A one-dimensional spatial setting similar to unstirred chemostat is used. The mortality rates of bacteria and grazers play important roles in the decomposition dynamics according to our mathematical analysis and sensitivity analysis.

Comparing to the system in [4], we consider the system with diffusion and discuss the influence of spatial heterogeneity on the dynamics of the system, which is more realistic for simulating the actual situation. Especially, the sign of the principal eigenvalue is a significant threshold for distinguishing the stability of the equilibrium, which is increasing as the diffusion rate increases and implies the diffusion rate also plays an important role in the stability of the equilibrium. The interaction of spatial heterogeneity and wave instability caused by the Hopf bifurcation may also lead to possible behavior such as long-wavelength traveling waves including spiral waves.

In the absence of grazing, the bacterial death rate completely determines asymptotic dynamics: bacteria become extinct when the death rate is large, and the bacterial density converges to a positive steady state when the death rate is small. On the other hand, in the presence of grazing, three kinds of dynamical behaviors appear: (i) extinction of both bacteria and grazers when the bacterial death rate is large; (ii) persistence of bacteria and extinction of grazers when the bacterial death rate is small and the grazer's death rate is large; and (iii) coexistence of bacteria and grazers when the death rates of bacteria and grazers are both small. See Corollary 5.3 and Fig. 5 for a precise description of parameter regimes. Moreover it is found that the coexistence of bacteria and grazers can be in an oscillatory fashion when the carbon input rate is large. In this case, the concentrations of bacteria and grazers change periodically and cannot sustain at a positive equilibrium for all the time, which creates a paradox of enrichment similar to the classical predator–prey model. The analytic results for the grazer–present system are proved under the assumption of equal diffusion coefficients, and the more realistic situation of unequal diffusion coefficients requires

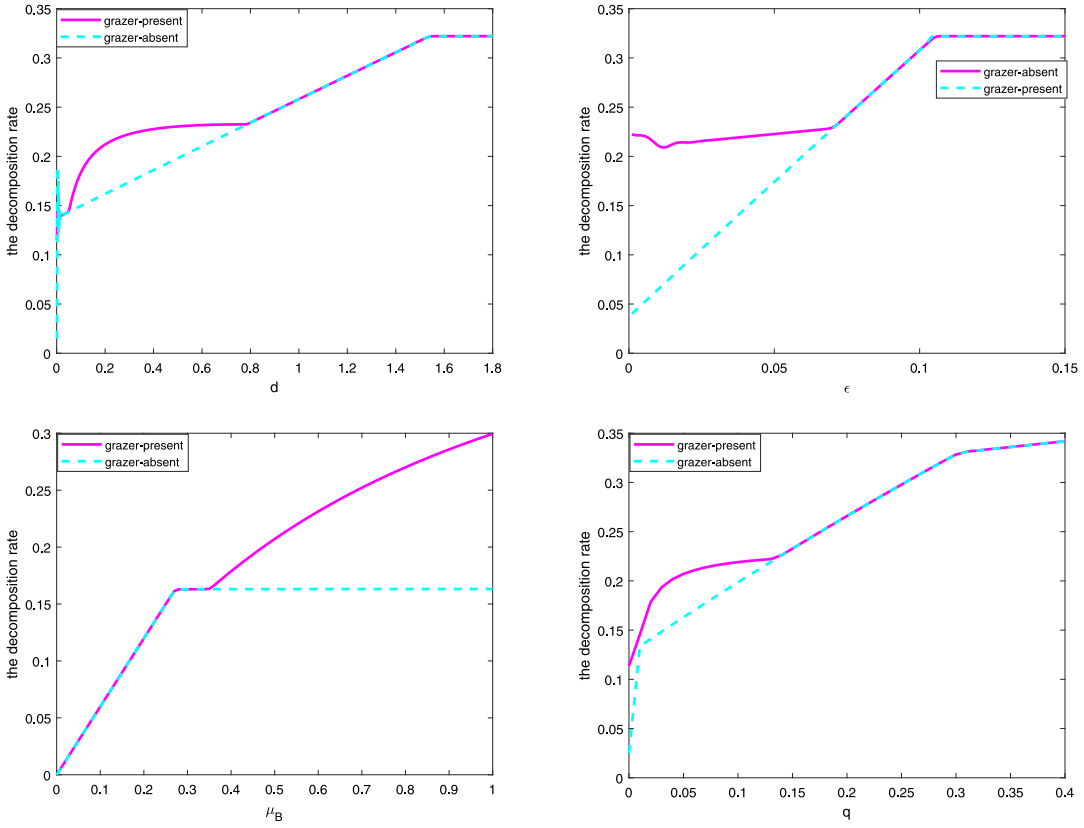

Fig. 13. The increase of the decomposition rate with respect to the parameter d, ϵ, μ_B or q. All parameter values except the bifurcation parameter are same as those in P_0. The magenta curves are for the grazer-present system and the cyan curves are for the grazer-absent system.

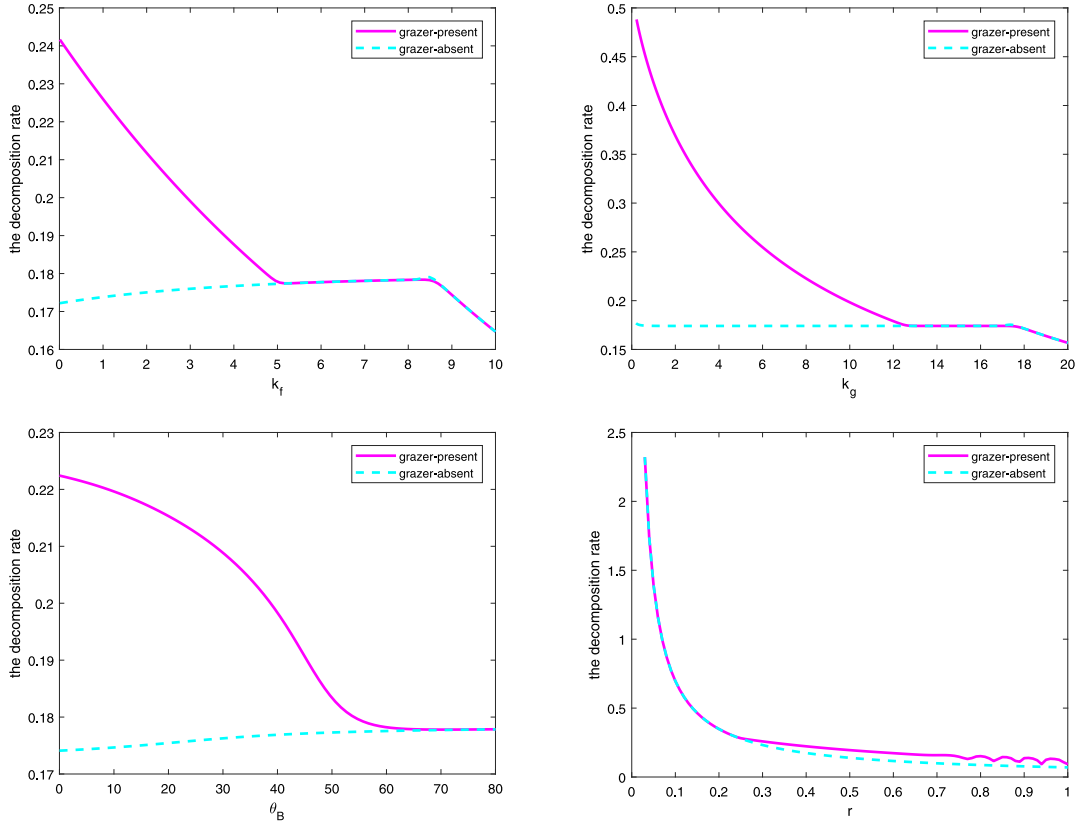

Fig. 14. The decrease of the decomposition rate with respect to the parameter k_f, k_g, θ_B or r. All parameter values except the bifurcation parameter are same as those in P_0. The magenta curves are for the grazer-present system and the cyan curves are for the grazer-absent system.

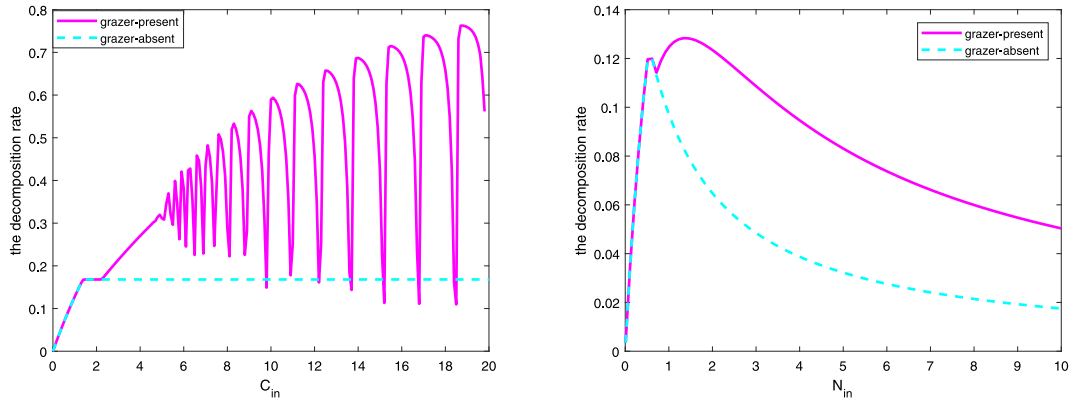

Fig. 15. The relationship between the decomposition rates and the parameters C_{in} and N_{in}. All parameter values except the bifurcation parameter are same as those in P_0. The magenta curves are for the grazer-present system and the cyan curves are for the grazer-absent system.

further future consideration. Numerical simulations in Figs. 7 and 10 show the dynamical behaviors for the system with unequal diffusion coefficients are similar to the one with equal diffusion coefficients.

The sensitivity of the degradation rate with respect to each parameter is shown numerically. The organic matter is decomposed to a greater extent and the decomposition rate is higher in the presence of grazers than in the absence of grazers in a resource-limited environment under some conditions. The relationship between the degradation rate and the parameters clearly explains the "decomposition–facilitation paradox" in a spatial setting. In some parameter ranges, the grazer's facilitation on biodegradation is negligible.

In [4], following the Liebig's law of minimum the non-smooth bacterial growth rate $\min\{f(N), g(C)\}$ was considered in the chemostat ODE system. The multiplication function used in this paper is a good approximation and has also been widely used in literature. For the reaction–diffusion model here, this simplification is necessary for rigorous mathematical analysis using the existing mathematical techniques. The rigorous analysis of a reaction–diffusion system with a non-smooth growth rate is an open mathematical question. The stability of interior steady states in the full grazer–present system is mathematically challenging and will be studied in the future.

Declaration of competing interest

The authors declare that they have no known competing financial interests or personal relationships that could have appeared to influence the work reported in this paper.

Acknowledgments

The authors would like to thank an anonymous reviewer for careful reading of the manuscript and for important suggestions and comments, which led to the improvement of our manuscript. This work was done when the first author visited Department of Mathematics, William & Mary during the academic year 2019–2020, and she would like to thank Department of Mathematics, William & Mary for their support and warm hospitality.

Appendix

Proof of Theorem 3.2. Let the total amount of nitrogen in the system be $P = \theta_B B + N + \theta_G G$ and the total amount of carbon in the system be $Q = B + C + G$, then $P(x,t)$ and $Q(x,t)$ satisfy

$$\begin{cases} P_t = dP_{xx}, & 0<x<L,\ t>0,\\ P_x(0,t) = -qN_{in}, \quad P_x(L,t) + qP(L,t) = 0, & t>0,\\ P(x,0) = \theta_B B^0(x) + N^0(x) + \theta_G G^0(x), & 0<x<L, \end{cases} \tag{A.1}$$

and

$$\begin{cases} Q_t = dQ_{xx} + \frac{\mu_B}{r}(r-1)\Phi(N,C)B + (\alpha-1)\mu_G h(B)G \le dQ_{xx}, & 0<x<L,\ t>0,\\ Q_x(0,t) = -qC_{in}, \quad Q_x(L,t) + qQ(L,t) = 0, & t>0,\\ Q(x,0) = B^0(x) + N^0(x) + C^0(x), & 0<x<L, \end{cases} \tag{A.2}$$

if $0 < r, \alpha \le 1$. Then $P(x,t)$ and $Q(x,t)$ satisfy

$$\lim_{t\to\infty} P(x,t) = \tilde{N}(x), \qquad \limsup_{t\to\infty} Q(x,t) \le \tilde{C}(x), \tag{A.3}$$

uniformly in $x \in [0, L]$, where $\tilde{N}(x)$ and $\tilde{C}(x)$ are the unique steady state solutions of diffusion equations in (A.1) and (A.2) with boundary conditions respectively. □

Proof of Proposition 4.1. The linearized equation of the limiting system (14) at $(0, \tilde{C}(x))$ is

$$\begin{cases} B_t = dB_{xx} + \mu_B\Phi(\tilde{N}(x),\tilde{C}(x))B - \epsilon B, & 0<x<L,\ t>0,\\ C_t = dC_{xx} - \frac{1}{r}\mu_B\Phi(\tilde{N}(x),\tilde{C}(x))B + \epsilon B, & 0<x<L,\ t>0,\\ B_x(0,t) = 0, \quad B_x(L,t) + qB(L,t) = 0, & t>0,\\ C_x(0,t) = -qC_{in}, \quad C_x(L,t) + qC(L,t) = 0, & t>0. \end{cases} \tag{A.4}$$

And the corresponding eigenvalue problem is

$$\begin{cases} d\phi_1'' + \mu_B\Phi(\tilde{N}(x),\tilde{C}(x))\phi_1 - \epsilon\phi_1 = \lambda\phi_1, & 0<x<L,\\ d\phi_2'' - \frac{1}{r}\mu_B\Phi(\tilde{N}(x),\tilde{C}(x))\phi_1 + \epsilon\phi_1 = \lambda\phi_2, & 0<x<L,\\ \phi_i'(0) = 0, \quad \phi_i'(L) + q\phi_i(L) = 0, & i = 1,2. \end{cases} \tag{A.5}$$

Let $(\lambda, \phi_1, \phi_2)$ be an eigen-pair of eigenvalue problem (A.5). If $\phi_1(x) \equiv 0$, then problem (A.5) is reduced to the one for ϕ_2, which is (11) with $p(x) = 0$, hence all eigenvalues are negative by Lemma 3.3. If $\phi_1(x) \not\equiv 0$, then problem (A.5) is reduced to the one for ϕ_1, which is (11) with $p(x) = \mu_B\Phi(\tilde{N}(x),\tilde{C}(x)) - \epsilon$. From Lemma 3.3, all eigenvalues are negative and $(0, \tilde{C}(x))$ is locally asymptotically stable if and only if (H_1) is satisfied, and $(0, \tilde{C}(x))$ is unstable if (H_2) is satisfied. □

To prove Theorem 4.2, we first prove the following auxiliary result.

Lemma A.1. *Assume* (H_1) *holds and* $0 < r \le 1$. *If* $V(x,t)$ *is the solution of*

$$\begin{cases} V_t = dV_{xx} + \mu_B\Phi(\tilde{N}(x) - \theta_B V, \tilde{C}(x) + \delta)V - \epsilon V, & 0<x<L,\ t>0,\\ V_x(0,t) = 0, \quad V_x(L,t) + qV(L,t) = 0, & t>0,\\ V(x,0) = B^0(x), & 0<x<L, \end{cases} \tag{A.6}$$

where $\delta > 0$ is a sufficiently small positive constant. Then

$$\lim_{t\to\infty} V(x,t) = 0, \quad \textit{uniformly for } x \in [0,L].$$

Proof. We construct another auxiliary function $v(x,t)$ satisfying

$$\begin{cases} v_t = d v_{xx} + \mu_B \Phi(\tilde{N}(x)+\delta, \tilde{C}(x)+\delta)v - \epsilon v, & 0 < x < L,\ t > T_0, \\ v_x(0,t) = 0, \qquad v_x(L,t) + q v(L,t) = 0, & t > T_0, \\ v(x,T_0) > V(x,T_0), & 0 < x < L. \end{cases}$$

where $T_0 > 0$ is defined in Theorem 3.2. Then by the comparison principle of parabolic equation, $v(x,t) > V(x,t)$ for $x \in [0,L]$ and $t \geq T_0$.

We prove that $v(x,t) \leq C_v e^{-\gamma(t-T_0)}$ for some positive constants C_v, sufficiently small $\gamma > 0$ and $t \geq T_0$, $0 \leq x \leq L$. Let $v(x,t) = y(x,t)\eta_0(x)e^{-\gamma(t-T_0)}$, where $\eta_0(x) > 0$ is the principal eigenfunction of (11) with $p(x) = \mu_B \Phi(\tilde{N}(x), \tilde{C}(x))$. Then $y(x,t)$ satisfies

$$\begin{cases} y_t - d y_{xx} - 2d\dfrac{\eta_0'}{\eta_0} y_x - \dfrac{y}{\eta_0} F = 0, & 0 < x < L,\ t > T_0, \\ y_x(0,t) = 0, \quad y_x(L,t) = 0, & t > T_0, \\ y(x,T_0) = \dfrac{v(x,T_0)}{\eta_0(x)}, & 0 < x < L, \end{cases} \tag{A.7}$$

where

$$\begin{aligned} F =& d\eta_0'' + \mu_B \Phi(\tilde{N}(x)+\delta, \tilde{C}(x)+\delta)\eta_0 + \gamma\eta_0 - \epsilon\eta_0 \\ =& (\epsilon^* - \epsilon)\eta_0 + \gamma\eta_0 + \mu_B(\Phi(\tilde{N}(x)+\delta, \tilde{C}(x)+\delta) - \Phi(\tilde{N}(x), \tilde{C}(x)))\eta_0 \\ <& 0, \end{aligned}$$

as $\gamma > 0$ and $\delta > 0$ are sufficiently small. Then from (A.7) we have

$$y_t - d y_{xx} - 2d\frac{\eta_0'}{\eta_0} y_x < 0.$$

Combining the boundary conditions in system (A.7) and the maximum principle, the maximum of y on $x \in [0,L]$ and $t \geq T_0$ should occur along $P_1 := \{t \geq T_0,\ x = 0\}$ or $P_2 := \{t \geq T_0,\ x = L\}$ or $P_3 := \{t = T_0,\ 0 < x < L\}$. If y has a nonnegative maximum $y(0,t)$ on P_1, then the Hopf boundary lemma implies that $y_x(0,t) < 0$ which is in contradiction with $y_x(0,t) = 0$. In the similar way, y cannot achieve a nonnegative maximum on P_2. Then the nonnegative maximum must lie on P_3. That is,

$$y(x,t) \leq y(x,T_0) \leq \sup_{x\in[0,L]} \frac{v(x,T_0)}{\eta_0(x)}.$$

Hence, any solution $V(x,t)$ of system (A.6) satisfies

$$V(x,t) \leq v(x,t) = y(x,t)\eta_0(x)e^{-\gamma(t-T_0)} \leq C_v e^{-\gamma(t-T_0)}$$

for some positive constant $C_v := \sup_{x\in[0,L]} \eta_0(x) \sup_{x\in[0,L]} \big(v(x,T_0)/\eta_0(x)\big)$. This implies that $V(x,t)$ converges to 0 uniformly for $x \in [0,L]$ as $t \to \infty$, which completes the proof. □

Now we prove Theorem 4.2.

Proof of Theorem 4.2. We only prove (i) as (ii) follows automatically from (i) and (A.3). From Theorem 3.2, for $t \geq T_0$ and $x \in [0,L]$, the solution $(B(x,t), C(x,t))$ of the limiting system (14) satisfies $B(x,t) \leq \tilde{C}(x) + \delta$ and $C(x,t) \leq \tilde{C}(x) + \delta$. By the comparison principle, we have the nonnegative solution $B(x,t)$ of the limiting system (14) is not larger than the nonnegative solution $V(x,t)$ of system (A.6), which leads to that $B(x,t) \to 0$ uniformly for $x \in [0,L]$ as $t \to \infty$ by Lemma A.1. From (A.3) we have $C(x,t) \to \tilde{C}(x)$ at the same time. □

Proof of Theorem 4.3. From the definitions, it is clear that $\mathbb{X}_0^2$ is an open subset in $\mathbb{X}^2$ and forward invariant under the dynamics generated by the limiting system (14). And $(0, \tilde{C}(x)) \in \partial\mathbb{X}_0^2$. We prove the remaining parts in several steps:

Step 1. $\Psi_t : \mathbb{X}_0^2 \to \mathbb{X}_0^2$ has a global attractor A_0.

Theorem 3.2 shows that Ψ_t is point dissipative on $\mathbb{X}^2$, and the forward orbits of bounded subsets of $\mathbb{X}^2$ for Ψ_t are bounded. Ψ_t is asymptotically smooth because it is compact from [31]. Then Ψ_t has a global attractor A_0 by [38].

Step 2. $\bigcup_{\theta\in N_\partial} \omega(\theta) \subset \{(0, \tilde{C}(x))\}$.

For any $\theta_0 \in N_\partial$ and $t \geq 0$, $\Psi(\theta_0) \in N_\partial$ by the definition of N_∂. Then $B(x,t,\theta_0) \equiv 0$ and $C(x,t,\theta_0)$ converges to $\tilde{C}(x)$ as $t \to \infty$ uniformly for $x \in [0,L]$. Hence, $\omega(\theta_0) \in \{(0, \tilde{C}(x))\}$.

Step 3. $\{(0, \tilde{C}(x))\}$ is a uniform weak repeller, that is, there exists a constant $\rho > 0$, such that for any $\theta \in \mathbb{X}_0^2$, $\limsup_{t\to\infty} \|\Psi_t(\theta) - (0, \tilde{C}(x))\| \geq \rho$.

On the contrary, if $(0, \tilde{C}(x))$ is not a weak repeller. Then for any $\rho > 0$, there exists $\theta^\rho = (B^\rho, C^\rho) \in \mathbb{X}_0^2$ such that $\limsup_{t\to\infty} \|\Psi_t(\theta^\rho) - (0, \tilde{C}(x))\| < \rho$. Especially, choose $\rho > 0$ such that $\lambda_0^\rho = \lambda_0(\mu_B \Phi(\tilde{N}(x) - \theta_B\rho, \tilde{C}(x) - \rho) - \epsilon) > 0$ is the principal eigenvalue of (11) with the corresponding eigenfunction $\eta_0^\rho > 0$. Thus, there exists $T_1 > 0$, such that for any $t \geq T_1$, $\|B(\cdot,t,\theta^\rho)\| < \rho$ and $\|C(\cdot,t,\theta^\rho) - \tilde{C}(\cdot)\| < \rho$. Therefore, for any $x \in [0,L]$ and $t \geq T_1$,

$$-\rho < B(x,t,\theta^\rho) < \rho, \quad \tilde{C} - \rho < C(x,t,\theta^\rho) < \tilde{C} + \rho.$$

On the other hand, from the limiting system (14),

$$\begin{aligned} B_t &= d B_{xx} + \mu_B \Phi(\tilde{N}(x) - \theta_B B, C)B - \epsilon B \\ &\geq d B_{xx} + (\mu_B \Phi(\tilde{N}(x) - \theta_B\rho, \tilde{C}(x) - \rho) - \epsilon)B, \end{aligned}$$

with the boundary condition $B_x(0,t) = B_x(L,t) + qB(L,t) = 0$. Choose $\xi_\rho > 0$ satisfying $B(x,T_1) \geq \xi_\rho \eta_0^\rho(x)$, then by the comparison principle, $B(x,t) \geq \xi_\rho \eta_0^\rho(x) e^{\lambda_0^\rho(t-T_1)}$ for any $t > T_1$, which implies $B(x,t)$ goes to ∞ as $t \to \infty$. This is in contradiction with $B(x,t) < \rho$.

Step 4. Define a continuous function $p : \mathbb{X}^2 \to [0,\infty)$ by $p(\theta) = \min_{x\in[0,L]} B(x)$ for any $\theta = (B,C) \in \mathbb{X}^2$. It is not difficult to see that $p^{-1}([0,\infty)) \subseteq \mathbb{X}_0^2$ and p satisfies that if $p(\theta) > 0$ or $\theta \in \mathbb{X}_0^2$ with $p(\theta) = 0$, then $p(\Psi_t(\theta)) > 0$ for $t > 0$, which implies that p is a generalized distance function for the semiflow $\Psi_t : \mathbb{X}^2 \to \mathbb{X}^2$.

To sum up the conclusions obtained above, it is true that any forward orbit of Ψ_t in N_∂ converges to $\{(0, \tilde{C}(x))\}$. $\{(0, \tilde{C}(x))\}$ is isolated in $\mathbb{X}^2$ and the stable set $W^s(\{(0, \tilde{C}(x))\})$ of $\{(0, \tilde{C}(x))\}$ satisfying $W^s(\{(0, \tilde{C}(x))\}) \cap \mathbb{X}_0^2 = \phi$. And there is no subsets of $\{(0, \tilde{C}(x))\}$ forms a cycle in N_∂. By applying the abstract persistence theory stated in [39–41], we have that there exists a constant $\varpi > 0$, such that $\min_{\theta^\varpi\in\omega(\theta)} p(\theta^\varpi) > \varpi$ for any $\theta \in \mathbb{X}_0^2$, which implies that for any $\theta \in \mathbb{X}_0^2$, $\liminf_{t\to\infty} B(\cdot,t,\theta) \geq \varpi$. □

Proof of Theorem 4.4. (i) We prove part (i) in four steps.

Step 1. $\dim \mathcal{N}(\mathcal{F}_{(B,C)}(\epsilon^*, 0, \tilde{C}(x))) = 1$, where $\mathcal{N}(\mathcal{F}_{(B,C)}(\epsilon^*, 0, \tilde{C}(x)))$ is the null space of the linear operator $\mathcal{F}_{(B,C)}(\epsilon^*, 0, \tilde{C}(x))$.

If $(\phi_1(x), \phi_2(x)) \in \mathcal{N}(\mathcal{F}_{(B,C)}(\epsilon^*, 0, \tilde{C}(x)))$, then we have

$$\begin{cases} d\phi_1''(x) + \mu_B \Phi(\tilde{N}(x), \tilde{C}(x))\phi_1(x) - \epsilon^*\phi_1(x) = 0, & 0 < x < L, \\ d\phi_2''(x) - \dfrac{1}{r}\mu_B \Phi(\tilde{N}(x), \tilde{C}(x))\phi_1(x) + \epsilon^*\phi_1(x) = 0, & 0 < x < L, \\ \phi_i'(0) = 0, \quad \phi_i'(L) + q\phi_i(L) = 0, & i = 1,2. \end{cases} \tag{A.8}$$

Since $\epsilon^* = \lambda_0(\mu_B \Phi(\tilde{N}(x), \tilde{C}(x)))$, then ϕ_1 can be chosen as η_0, and ϕ_2 can be uniquely solved from the second equation of (A.8) as expressed in (19). Hence

$$\dim \mathcal{N}(\mathcal{F}_{(B,C)}(\epsilon^*, 0, \tilde{C}(x))) = 1, \quad \mathcal{N}(\mathcal{F}_{(B,C)}(\epsilon^*, 0, \tilde{C}(x))) = \operatorname{span}\{(\eta_0, \zeta_0)\}.$$

Step 2. $\operatorname{codim} \mathcal{R}(\mathcal{F}_{(B,C)}(\epsilon^*, 0, \tilde{C}(x))) = 1$, where $\mathcal{R}(\mathcal{F}_{(B,C)}(\epsilon^*, 0, \tilde{C}(x)))$ is the range of the linear operator $\mathcal{F}_{(B,C)}(\epsilon^*, 0, \tilde{C}(x))$.

Assume $(u_1, u_2, u_3) \in \mathcal{R}(\mathcal{F}_{(B,C)}(\epsilon^*, 0, \tilde{C}(x)))$, then there exists $(\varphi_1, \varphi_2) \in \mathbb{X}_B \times \mathbb{X}_C$ such that

$$\begin{cases} d\varphi_1''(x) + \mu_B \Phi(\tilde{N}(x), \tilde{C}(x))\varphi_1(x) - \epsilon^*\varphi_1(x) = u_1, & 0 < x < L, \\ d\varphi_2''(x) - \dfrac{1}{r}\mu_B \Phi(\tilde{N}(x), \tilde{C}(x))\varphi_1(x) + \epsilon^*\varphi_1(x) = u_2, & 0 < x < L, \\ \varphi_1'(0) = 0, \quad \varphi_1'(L) + q\varphi_1(L) = 0, \\ \varphi_2'(0) = u_3, \quad \varphi_2'(L) + q\varphi_2(L) = 0. \end{cases} \tag{A.9}$$

Multiplying φ_1 and ϕ_1 to the first equation of (A.8) and (A.9), respectively, subtracting and integrating over $[0, L]$, we obtain $\int_0^L u_1(x)\phi_1(x)dx = 0$, and φ_2 is always solvable for any (u_2, u_3), which implies that

$$\mathcal{R}(\mathcal{F}_{(B,C)}(\epsilon^*, 0, \tilde{C}(x))) = \left\{ (u_1, u_2, u_3)^T \in \mathbb{Y}\times\mathbb{Y}\times\mathbb{R} : \int_0^L u_1(x)\eta_0(x)dx = 0 \right\}$$

and $\operatorname{codim} \mathcal{R}(\mathcal{F}_{(B,C)}(\epsilon^*, 0, \tilde{C}(x))) = 1$.

Step 3. $\mathcal{F}_{\epsilon(B,C)}(\epsilon^*, 0, \tilde{C}(x))[(\eta_0, \zeta_0)] \notin \mathcal{R}(\mathcal{F}_{(B,C)}(\epsilon^*, 0, \tilde{C}(x)))$.

A direct calculation shows that $\mathcal{F}_{\epsilon(B,C)}(\epsilon^*, 0, \tilde{C}(x))[(\eta_0, \zeta_0)] = (-\eta_0, \eta_0, 0)$. Assume $(-\eta_0, \eta_0, 0)^T \in \mathcal{R}(\mathcal{F}_{(B,C)}(\epsilon^*, 0, \tilde{C}(x)))$. Then $\int_0^L \eta_0^2(x)dx = 0$, which is in contradiction with $\eta_0 > 0$.

Step 4. Now applying the Theorem 1.7 of [42], we have that there exists $I = (-\sigma, \sigma)$ for $0 < \sigma \ll 1$, and $\epsilon : I \to \mathbb{R}$, $w_i : I \to \mathbb{W}$ $(i = 1, 2)$, where $\mathbb{W}$ is a complement of $\operatorname{span}\{(\eta_0, \zeta_0)\}$, such that the set of solutions of the limiting system (18) near $(\epsilon^*, 0, \tilde{C}(x))$ consists precisely of the smooth curve $\Gamma_0 = \{(\epsilon, 0, \tilde{C}(x)) : 0 < \epsilon < \epsilon^*\}$ and $\Gamma_1 = \{(\epsilon(s), B(s, x), C(s, x)) : s \in I\backslash\{0\}\}$. Restricting $s \in (0, \sigma)$, we obtain the branch Γ_1^+ of positive solutions of (18) as stated in part (i).

(ii) For part (ii), we can calculate that (see [43])

$$\epsilon'(0) = -\frac{\langle \kappa, \mathcal{F}_{(B,C)(B,C)}(\epsilon^*, 0, \tilde{C}(x))[(\eta_0, \zeta_0), (\eta_0, \zeta_0)]\rangle}{2\langle \kappa, F_{\epsilon(B,C)}(\epsilon^*, 0, \tilde{C}(x))[(\eta_0, \zeta_0)]\rangle} = -\frac{\mu_B \int_0^L \left(\theta_B \Phi_N(\tilde{N}(x), \tilde{C}(x))\eta_0(x) - \Phi_C(\tilde{N}(x), \tilde{C}(x))\zeta_0(x)\right)\eta_0^2(x)\mathrm{d}x}{\int_0^L \eta_0^2(x)\mathrm{d}x},$$

as

$$\mathcal{F}_{(B,C)(B,C)}(\epsilon^*, 0, \tilde{C}(x))[(\eta_0, \zeta_0), (\eta_0, \zeta_0)] = \begin{pmatrix} -2\mu_B\theta_B\Phi_N(\tilde{N}(x), \tilde{C}(x))\eta_0^2(x) + 2\mu_B\Phi_C(\tilde{N}(x), \tilde{C}(x))\eta_0(x)\zeta_0(x) \\ 2\frac{\mu_B}{r}\theta_B\Phi_N(\tilde{N}(x), \tilde{C}(x))\eta_0^2(x) - 2\frac{\mu_B}{r}\Phi_C(\tilde{N}(x), \tilde{C}(x))\eta_0(x)\zeta_0(x) \\ 0 \end{pmatrix},$$

$F_{\epsilon(B,C)}(\epsilon^*, 0, \tilde{C}(x))[\rho_0] = (-\eta_0, \eta_0, 0)$, $\kappa = (\eta_0, 0, 0)$.

Since $(\eta_0(x), \zeta_0(x))$ is a solution of (A.8), it leads to that

$$\eta_0(x) + \zeta_0(x) = (-d\Delta)^{-1}\left(\frac{\mu_B}{r}(r-1)\Phi(\tilde{N}(x), \tilde{C}(x))\eta_0(x)\right) \le 0,$$

since $0 < r \le 1$. This implies $\zeta_0(x) \le -\eta_0(x) < 0$, hence $\epsilon'(0) < 0$ as $\Phi_N > 0$ and $\Phi_C > 0$. By applying the stability theorem of bifurcating solutions in [42], there exists up to the second order continuous differentiable functions:

$$\nu : (\epsilon^* - \sigma, \epsilon^* + \sigma) \to \mathbb{R}, \quad (\hat{B}(\tau), \hat{C}(\tau)) : (\epsilon^* - \sigma, \epsilon^* + \sigma) \to \mathbb{X}_B \times \mathbb{X}_C,$$
$$\mu : (-\xi, \xi) \to \mathbb{R}, \quad (B^*, C^*) : (-\xi, \xi) \to \mathbb{X}_B \times \mathbb{X}_C,$$

such that

$$\mathcal{F}_{(B,C)}(\epsilon, 0, \tilde{C}(x))[\hat{B}(\tau), \hat{C}(\tau)] = \nu(\tau)[\hat{B}(\tau), \hat{C}(\tau), 0]^T,$$
$$\mathcal{F}_{(B,C)}(\epsilon(s), B(s), C(s))[B^*(s), C^*(s)] = \mu(s)[B^*(s), C^*(s), 0]^T,$$

where $\nu(\epsilon) = \epsilon^* - \epsilon$, $\nu'(\epsilon^*) = -1$, and $\mu(s)$ has the same sign of $-s\epsilon'(s)\nu'(\epsilon^*)$ when s is small, which implies $\mu(s) < 0$ and the bifurcating solution $(\epsilon(s), B(s, x), C(s, x))$ is locally asymptotically stable with respect to (14). □

Proof of Theorem 4.5. From Theorem 3.3 and Remark 3.4 of [33], it is not difficult to verify that for any fixed $(\bar{B}, \bar{C}) \in \mathbb{X}_B \times \mathbb{X}_C$, the operator $\mathcal{F}_{(B,C)}(\epsilon, \bar{B}, \bar{C}) : \mathbb{X}_B \times \mathbb{X}_C \to \mathbb{Y}\times\mathbb{Y}\times\mathbb{R}$ is a Fredholm operator with index zero. Then the existence of $\mathcal{C}$ follows from Theorem 4.3 of [33], and the existence of $\mathcal{C}^+$ follows from Theorem 4.4 of [33]. Moreover from Theorem 4.4 in [33], $\mathcal{C}^+$ must satisfy one of the following alternatives:

(i) it is not compact in $\mathbb{R}_+ \times \mathbb{X}_B \times \mathbb{X}_C$;
(ii) it contains a point $(\hat{\epsilon}, 0, \tilde{C}(x))$ with $\hat{\epsilon} \ne \epsilon^*$;
(iii) it contains a point $(\epsilon, \bar{B}(s, x), \tilde{C}(x) + \bar{C}(s, x))$, where $(\bar{B}(s, x), \bar{C}(s, x)) \ne (0, 0)$, $(\bar{B}(s, x), \bar{C}(s, x)) \in \mathbb{W}$, and $\mathbb{W}$ is a complement of $\operatorname{span}\{(\eta_0, \zeta_0)\}$ defined in the proof of Theorem 4.4.

To show case (ii) cannot happen, we prove that $\epsilon = \epsilon^*$ is the unique bifurcation value for the bifurcation of positive solutions of (18) from Γ_0. We prove it by contradiction. Suppose that $\hat{\epsilon}$ $(\ne \epsilon^*)$ is another bifurcation value for the bifurcation of positive solutions of (18) from Γ_0, then there exists a sequence of positive solutions $\{(\epsilon_n, B_n(x), C_n(x))\}_{n=1}^{\infty}$ such that $(\epsilon_n, B_n(x), C_n(x)) \to (\hat{\epsilon}, 0, \tilde{C}(x))$ as $n \to \infty$ for some $\hat{\epsilon} > 0$. Let $b_n = \frac{B_n}{\|B_n\|}$. Then b_n satisfies

$$db_n'' + \mu_B\Phi(\tilde{N}(x) - \theta_B B_n, C_n)b_n - \epsilon_n b_n = 0,$$

with the same boundary condition. From standard elliptic estimates, there exists a subsequence of $\{b_n\}_{n=1}^{\infty}$, still denoted as itself, such that $b_n \to b_\infty \in \mathbb{X}_B$, $b_\infty \ge 0$ and $\|b_\infty\| = 1$. Moreover b_∞ satisfies

$$\begin{cases} db_\infty'' + \mu_B\Phi(\tilde{N}(x), \tilde{C}(x))b_\infty - \hat{\epsilon}b_\infty = 0, & 0 < x < L, \\ b_\infty'(0) = 0, \quad b_\infty'(L) + qb_\infty(L) = 0. \end{cases} \tag{A.10}$$

Hence $\hat{\epsilon} = \lambda_i(\mu_B\Phi(\tilde{N}(x), \tilde{C}(x)))$ for some $i \ge 0$. But from Lemma 3.3, λ_0 is the only eigenvalue with a nonnegative eigenfunction, thus $\hat{\epsilon} = \lambda_0(\mu_B\Phi(\tilde{N}(x), \tilde{C}(x))) = \epsilon^*$. That is a contradiction. So $\epsilon = \epsilon^*$ is the unique bifurcation value for positive solutions of (18) from Γ_0. Hence case (ii) cannot happen.

If case (iii) holds, then there exists $\bar{\epsilon} \in (0, \epsilon^*)$, such that $(\bar{B}(s, x), \tilde{C}(x) + \bar{C}(s, x))$ is positive and satisfies $\mathcal{F}(\bar{\epsilon}, \bar{B}(s, x), \tilde{C}(x) + \bar{C}(s, x)) = 0$ and $(\bar{B}(s, x), \bar{C}(s, x)) \in \mathbb{W}$, i.e.

$$\int_0^L (\bar{B}(s, x)\eta_0(x) + \bar{C}(s, x)\zeta_0(x))\mathrm{d}x = 0, \tag{A.11}$$

where $\eta_0(x) > 0$ and $\zeta_0(x) < 0$ are defined in Theorem 4.4. On the other hand, $\tilde{C}(x) + \bar{C}(s, x) \le \tilde{C}(x)$ from the maximum principle. Then $\bar{C}(s, x) \le 0$ and $\int_0^L (\bar{B}(s, x)\eta_0(x) + \bar{C}(s, x)\zeta_0(x))\mathrm{d}x > 0$, which is in contradiction with (A.11). Hence, (iii) cannot happen and (i) must occur. From the maximum principle, we have $B(x) \le \max_{x\in[0,L]} \tilde{B}(x)$ and $C(x) \le (1 + qL)C_{in}$, so all solutions (B, C) on $\mathcal{C}^+$ are uniformly bounded, and positive solutions of system (18) only exist when $\epsilon < \epsilon^*$. Therefore we must have $\operatorname{Proj}_\epsilon \mathcal{C}^+ = (0, \epsilon^*)$. □

Proof of Theorem 5.1. The eigenvalue problem of the linearized equation of (20) at E_0 is

$$\begin{cases} d\phi_1'' + \mu_B\Phi(\tilde{N}(x), \tilde{C}(x))\phi_1 - \epsilon\phi_1 = \lambda\phi_1, & 0 < x < L, \\ d\phi_2'' - \frac{1}{r}\mu_B\Phi(\tilde{N}(x), \tilde{C}(x))\phi_1 + \epsilon\phi_1 + \beta\phi_3 = \lambda\phi_2, & 0 < x < L, \\ d\phi_3'' - \beta\phi_3 = \lambda\phi_3, & 0 < x < L, \\ \phi_i'(0) = 0, \quad \phi_i'(L) + q\phi_i(L) = 0, & i = 1, 2, 3. \end{cases} \tag{A.12}$$

Let $(\lambda, \phi_1, \phi_2, \phi_3)$ be an eigen-pair of eigenvalue problem (A.12). If $\phi_1(x) \equiv 0$ and $\phi_3(x) \equiv 0$, then problem (A.12) is reduced to the one for ϕ_2, which is (11) with $p(x) = 0$, hence all eigenvalues are negative by Lemma 3.3. If $\phi_3(x) \not\equiv 0$, then problem (A.12) is reduced to the one for ϕ_3, which is (11) with $p(x) = -\beta$, hence all eigenvalues are negative by Lemma 3.3. If $\phi_1(x) \not\equiv 0$, then problem (A.12) is reduced to the one for ϕ_1, which is (11) with $p(x) = \mu_B\Phi(\tilde{N}(x), \tilde{C}(x)) - \epsilon$. From Lemma 3.3, all eigenvalues are negative and $(0, \tilde{C}(x))$ is locally asymptotically stable if and only if (H_1) is satisfied, and $(0, \tilde{C}(x))$ is unstable if (H_2) is satisfied. Hence E_0 is locally asymptotically stable if (H_1) holds and is unstable if (H_2) holds. The existence of E_1 under (H_2) follows from Theorem 4.5.

Next we prove that when (H_1) holds, if $(B(x, t), C(x, t), G(x, t))$ is a nonnegative solution of the limiting system (20), then

$$\lim_{t\to\infty}(B(x, t), C(x, t), G(x, t)) = (0, \tilde{C}(x), 0), \quad \text{uniformly for } x \in [0, L].$$

From Theorem 3.2, for any constant $0 < \delta \ll 1$, there exists a $T_1 > 0$, such that

$$B_t = dB_{xx} + \mu_B\Phi(\tilde{N}(x) - \theta_B B - \theta_G G, C)B - \mu_G h(B)G - \epsilon B \le dB_{xx} + \mu_B\Phi(\tilde{N}(x) - \theta_B B, \tilde{C}(x) + \delta)B - \epsilon B,$$

for any $x \in [0, L]$ and $t \geq T_1$. Thus, by the comparison principle and Lemma A.1, if $0 < r \leq 1$ and (H_1) hold, then $\lim_{t\to\infty} B(x,t) = 0$ uniformly for $x \in [0, L]$. Hence there exists $T_2 > 0$ such that for $t > T_2$, $B(x,t) \leq \delta$ for all $x \in [0, L]$. From the third equation of system (20), we have $G_t \leq dG_{xx} + (\alpha\mu_G h(\delta) - \beta)G$ for $t > T_2$. Choosing δ small enough so that $\alpha\mu_G h(\delta) - \beta < -\beta/2$, we have $G_t < dG_{xx} - \beta G/2$, which implies $\lim_{t\to\infty} G(x,t) = 0$ uniformly for $x \in [0, L]$. As $(B(x,t), G(x,t))$ goes to $(0,0)$ when $t \to \infty$, $C(x,t)$ converges to $\tilde{C}(x)$ at the same time by the continuity of solution map, which proves the convergence to E_0.

Finally we prove that E_1 is locally asymptotically stable when $\epsilon^* - \sigma < \epsilon < \epsilon^*$. Let $(\lambda, \phi_1, \phi_2, \phi_3)$ be an eigen-pair of the following eigenvalue problem corresponding to the linearized equation of (20) at E_1:

$$\begin{cases} d\phi_1'' - \epsilon\phi_1 - \mu_B\theta_B\Phi_N(\tilde{E}_1)B_1\phi_1 - \mu_G h(B_1)\phi_3 + \mu_B\Phi(\tilde{E}_1)\phi_1 \\ \quad +\mu_B\Phi_C(\tilde{E}_1)B_1\phi_2 - \mu_B\theta_B\Phi_N(\tilde{E}_1)B_1\phi_3 = \lambda\phi_1, & 0 < x < L, \\ d\phi_2'' + \frac{\mu_B\theta_B}{r}\Phi_N(\tilde{E}_1)B_1\phi_1 + \epsilon\phi_1 - \frac{\mu_B}{r}\Phi(\tilde{E}_1)\phi_1 + \beta\phi_3 \\ \quad -\frac{\mu_B}{r}\Phi_C(\tilde{E}_1)B_1\phi_2 + \frac{\mu_B\theta_B}{r}\Phi_N(\tilde{E}_1)B_1\phi_3 = \lambda\phi_2, & 0 < x < L, \\ d\phi_3'' + (\alpha\mu_G h(B_1) - \beta)\phi_3 = \lambda\phi_3, & 0 < x < L, \\ \phi_i'(0) = 0, \qquad \phi_i'(L) + q\phi_i(L) = 0, & i = 1, 2, 3, \end{cases} \tag{A.13}$$

where $\tilde{E}_1 = (\tilde{N}(x) - \theta_B B_1(x), C_1(x))$. If $\phi_3(x) \not\equiv 0$, then problem (A.13) is reduced to the one for ϕ_3, which is (11) with $p(x) = \alpha\mu_G h(B_1(x)) - \beta$, hence all eigenvalues are negative provided $\lambda_0(\alpha\mu_G h(B_1(x))) - \beta < 0$. Since $\lim_{\epsilon\to} (\epsilon^*)^- \lambda_0(\alpha\mu_G h(B_1(x))) = \lambda_0(0) < 0$, we can choose $\sigma > 0$ small enough so that $\lambda_0(\alpha\mu_G h(B_1(x))) - \beta < 0$ holds for positive $\beta > 0$ and $\epsilon^* - \sigma < \epsilon < \epsilon^*$. If $\phi_3(x) \equiv 0$, then problem (A.13) is reduced to the one for ϕ_1 and ϕ_2. From the proof of Theorem 4.4, all eigenvalues are negative when $\epsilon^* - \sigma < \epsilon < \epsilon^*$. Hence, we obtain that E_1 is locally asymptotically stable when $\epsilon^* - \sigma < \epsilon < \epsilon^*$ and $\lambda_0(\alpha\mu_G h(B_1(x))) - \beta < 0$. □

To prove Theorem 5.2, we first prove several lemmas.

Lemma A.2. *The function* $m(x) = \alpha\mu_G \inf_{B\in\mathcal{P}(A_0)}(h(B(x))$ *is continuous on* $[0, L]$.

Proof. We prove it by using the definition of continuous functions. That is, for any $\varepsilon > 0$, there exists $\delta > 0$, such that for any $x, y \in [0, L]$ satisfying $|x - y| < \delta$, we have $|m(x) - m(y)| < \varepsilon$, or equivalently, $m(y) - \varepsilon < m(x) < m(y) + \varepsilon$.

From the mean-value theorem, we have

$$|h(B(x)) - h(B(y))| = |h'(B(\sigma x + (1-\sigma)y))| \cdot |x - y| \leq \frac{1}{k_h}|x - y|,$$

where $\sigma \in (0, 1)$. Then for any $\varepsilon > 0$, there exist $\delta = \varepsilon k_h/(2\alpha\mu_G) > 0$, such that for any $(x, B), (y, B) \in [0, 1] \times \mathcal{P}(A_0)$ satisfying $|x - y| < \delta$, $|h(B(x)) - h(B(y))| < \varepsilon/(2\alpha\mu_G)$. That is,

$$h(B(x)) - \frac{\varepsilon}{2\alpha\mu_G} \leq h(B(y)) \leq h(B(x)) + \frac{\varepsilon}{2\alpha\mu_G}.$$

From the definition of $m(x)$, we have that

$$m(x) = \alpha\mu_G \inf_{B\in\mathcal{P}(A_0)} h(B(x)), \qquad m(y) = \alpha\mu_G \inf_{B\in\mathcal{P}(A_0)} h(B(y)).$$

Then there exist $B^x, B^y \in \mathcal{P}(A_0)$, such that $m(x) + \varepsilon/2 > \alpha\mu_G h(B^x(x))$ and $m(y) + \varepsilon/2 > \alpha\mu_G h(B^y(y))$. Thus,

$$m(x) + \frac{\varepsilon}{2} > \alpha\mu_G h(B^x(x)) > \alpha\mu_G h(B^x(y)) - \frac{\varepsilon}{2} \geq m(y) - \frac{\varepsilon}{2},$$

and

$$m(y) + \frac{\varepsilon}{2} > \alpha\mu_G h(B^y(y)) > \alpha\mu_G h(B^y(x)) - \frac{\varepsilon}{2} \geq m(x) - \frac{\varepsilon}{2}.$$

Hence, $m(x)$ is uniformly continuous on $[0, L]$, which completes the proof. □

Lemma A.3. *Assume* (H_2) *holds and* $0 < r, \alpha \leq 1$. *If* (H_3) *holds, then* $M_0 = \{E_0\}$ *and* $M_1 = A_0 \times \{0\}$ *are uniform weak repellers with respect to* $(\mathbb{X}_1^3, \partial\mathbb{X}_1^3)$, *that is, there exists a constant* $\tilde{p} > 0$, *such that for any* $\Theta^0 \in \mathbb{X}_1^3$,

$$\limsup_{t\to\infty} \operatorname{dist}(\widetilde{\Psi}_t(\Theta^0), M_i) \geq \tilde{p}, \qquad i = 0, 1.$$

Proof. It is proved by contradiction. Suppose, in contrary, M_0 and M_1 are not weak repellers. Then there exists $\Theta^{\tau_0} = (B^{\tau_0}, C^{\tau_0}, G^{\tau_0}) \in \mathbb{X}_1^3$, such that

$$\limsup_{t\to\infty} \operatorname{dist}(\widetilde{\Psi}_t(\Theta^{\tau_0}), M_0) < \tau_0, \qquad \limsup_{t\to\infty} \operatorname{dist}(\widetilde{\Psi}_t(\Theta^{\tau_0}), M_1) < \tau_0.$$

Hence there exists $T_3 > 0$, such that for any $t > T_3$,

$$\|G(\cdot, t, G^{\tau_0})\| < \tau_0, \tag{A.14}$$

which implies that $-\tau_0 < G(\cdot, t, G^{\tau_0}) < \tau_0$.

On the other hand, from system (20), we have

$$G_t = dG_{xx} + (\alpha\mu_G h(B) - \beta)G \geq dG_{xx} + (m(x) - \beta)G.$$

Let $\eta_0^m(x) > 0$ be the principal eigenfunction corresponding to the principal eigenvalue $\lambda_0(m(x) - \beta)$. Then by the comparison principle, $G(x, t, G^{\tau_0}) \geq \xi_m \eta_0^m(x) e^{\lambda_0(m(x)-\beta)(t-T_3)}$ for all $x \in [0, L]$ and a constant $\xi_m > 0$. Thus, as $t \to \infty$, $G(x, t, G^{\tau_0})$ goes to ∞, which is in contradiction with (A.14). □

Lemma A.4. *Assume* (H_2) *holds and* $0 < r, \alpha \leq 1$. *Then for any* $\Theta^0 \in N_\partial^1$, $\widetilde{\omega}(\Theta^0) \subset M_0 \cup M_1$.

Proof. For any $\Theta^0 \in N_\partial^1$, we have $\widetilde{\Psi}_t(\Theta^0) \in \partial\mathbb{X}_1^3$ and $\widetilde{\Psi}_t(\Theta^0) \in N_\partial^1$. Then for any $t \geq 0$ and $x \in [0, L]$, $B(x, t, \Theta^0) \equiv 0$ or $G(x, t, \Theta^0) \equiv 0$. If $B(x, t, \Theta^0) \equiv 0$, then $G(x, t, \Theta^0) \equiv 0$, and $C(x, t, \Theta^0)$ converges to $\tilde{C}(x, \Theta^0)$ uniformly as t goes to ∞. Hence, $\lim_{t\to\infty} \widetilde{\Psi}_t(\Theta^0) = E_0$ and $\widetilde{\omega}(\Theta^0) \subset M_0$.

Assume $G(x, t, \Theta^0) \equiv 0$ for all $t \geq 0$ and $x \in [0, L]$. Substituting it into system (20), $(B(x, t, \Theta^0), C(x, t, \Theta^0))$ satisfies the limiting system (14). By Theorem 4.3, A_0 is a global attractor of Ψ_t, then $(B(x, t, \Theta^0), C(x, t, \Theta^0))$ will eventually enter $A_0 \subset \operatorname{Int}(\mathbb{X}^2)$. Thus, $\widetilde{\Psi}_t(\Theta^0)$ will eventually enter the global attractor M_1 and $\widetilde{\omega}(\Theta^0) \subset M_1$. □

Now, we are in position to prove Theorem 5.2.

Proof of Theorem 5.2. It is easy to see that if the initial condition $(B^0, C^0, G^0) \in \mathbb{X}_1^3$, then we have $B(x, t, B^0(x)) > 0$ and $G(x, t, G^0(x)) > 0$ for all $x \in [0, L]$ and $t > 0$, which implies that $\widetilde{\Psi}_t(\mathbb{X}_1^3) \subset \mathbb{X}_1^3$ for all $t > 0$. The semiflow $\widetilde{\Psi}_t : \mathbb{X}^3 \to \mathbb{X}^3$ has a global attractor in $\mathbb{X}^3$ from Theorem 3.2 and [38]. The sets M_0 and M_1 are isolated in $\mathbb{X}^3$, and no subset of M_0 and M_1 forms a cycle in $\partial\mathbb{X}_1^3$ by Lemmas A.3 and A.4. Also, the stable set $W^s(M_i)$ of M_i satisfies $W^s(M_i) \cap \mathbb{X}_1^3 = \phi$ for $i = 0, 1$.

Define a continuous function $D : \mathbb{X}^3 \to [0, \infty)$ as

$$D(\Theta^0) = \min\left\{\min_{x\in[0,L]} B^0(x), \min_{x\in[0,L]} G^0(x)\right\}, \qquad \Theta^0 = (B^0, C^0, G^0) \in \mathbb{X}_1^3.$$

Then D is a generalized distance function for $\widetilde{\Psi}_t$, and there exists a constant $\varpi_1 > 0$, such that $\min_{\Theta\in\widetilde{\omega}(\Theta^0)} D(\Theta) > \varpi_1$ for $\Theta^0 \in \mathbb{X}_1^3$, and the uniform persistence is valid. By [38], it shows that $\widetilde{\Psi}_t : \mathbb{X}_1^3 \to \mathbb{X}_1^3$ has a global attractor A_1 and that $\widetilde{\Psi}_t$ has a steady state $(B_2, C_2, G_2) \in A_1$. □

References

[1] S. Das, P.S. Lyla, S.A. Khan, Marine microbial diversity and ecology: importance and future perspectives, Current Sci. 90 (2006) 1325–1335.

[2] S. Das, H.R. Dash, Microbial bioremediation: a potential tool for restoration of contaminated areas, in: Microbial Biodegradation and Bioremediation, Elsevier, 2014, pp. 1–21.

[3] J.D. Kong, H. Wang, T. Siddique, J. Foght, K. Semple, Z. Burkus, M.A. Lewis, Second-generation stoichiometric mathematical model to predict methane emissions from oil sands tailings, Sci. Total Environ. 694 (2019) 133645.

[4] J.D. Kong, P. Salceanu, H. Wang, A stoichiometric organic matter decomposition model in a chemostat culture, J. Math. Biol. 76 (3) (2018) 609–644.

[5] H. Wang, L. Jiang, J.S. Weitz, Bacterivorous grazers facilitate organic matter decomposition: a stoichiometric modeling approach, FEMS Microbiol. Ecol. 69 (2) (2009) 170–179.
[6] T. Fenchel, P. Harrison, The significance of bacterial grazing and mineral cycling for decomposition of particulate debris, in: Terrestrial and Aquatic Organisms in Decomposition Processes, Blackwell Sci. Pub., Oxford, 1976, pp. 285–299.
[7] L. Jiang, Negative selection effects suppress relationships between bacterial diversity and ecosystem functioning, Ecology 88 (5) (2007) 1075–1085.
[8] B. Nisbet, Nutrition and Feeding Strategies in Protozoa, Springer, 1984.
[9] C.H. Ratsak, K.A. Maarsen, S.A.L.M. Kooijman, Effects of protozoa on carbon mineralization in activated sludge, Water Res. 30 (1) (1996) 1–12.
[10] B.F. Sherr, E.B. Sherr, C.S. Hopkinson, Trophic interactions within pelagic microbial communities: indications of feedback regulation of carbon flow, Hydrobiologia 159 (1) (1988) 19–26.
[11] M.L. Rosenzweig, Paradox of enrichment: destabilization of exploitation ecosystems in ecological time, Science 171 (3969) (1971) 385–387.
[12] G. Bratbak, Bacterial biovolume and biomass estimations, Appl. Environ. Microbiol. 49 (6) (1985) 1488–1493.
[13] B.W. Kooi, M.P. Boer, S.A.L.M. Kooijman, Complex dynamic behaviour of autonomous microbial food chains, J. Math. Biol. 36 (1) (1997) 24–40.
[14] P.A. Del Giorgio, J.J. Cole, Bacterial growth efficiency in natural aquatic systems, Annu. Rev. Ecol. Syst. 29 (1) (1998) 503–541.
[15] H. Wang, H.L. Smith, Y. Kuang, J.J. Elser, Dynamics of stoichiometric bacteria-algae interactions in the epilimnion, SIAM J. Appl. Math. 68 (2) (2007) 503–522.
[16] R.W. Sterner, J.J. Elser, Ecological Stoichiometry: The Biology of Elements from Molecules to the Biosphere, Princeton university press, 2002.
[17] W.F. Cross, J.P. Benstead, P.C. Frost, S.A. Thomas, Ecological stoichiometry in freshwater benthic systems: recent progress and perspectives, Freshwater Biol. 50 (11) (2005) 1895–1912.
[18] H. Wang, Z.-X. Lu, A. Raghavan, Weak dynamical threshold for the "strict homeostasis" assumption in ecological stoichiometry, Ecol. Model. 384 (2018) 233–240.
[19] H. Wang, R.W. Sterner, J.J. Elser, On the "strict homeostasis" assumption in ecological stoichiometry, Ecol. Model. 243 (2012) 81–88.
[20] S.-B. Hsu, F.-B. Wang, X.-Q. Zhao, A reaction-diffusion model of harmful algae and zooplankton in an ecosystem, J. Math. Anal. Appl. 451 (2) (2017) 659–677.
[21] R.H. Martin Jr., H.L. Smith, Abstract functional-differential equations and reaction-diffusion systems, Trans. Amer. Math. Soc. 321 (1) (1990) 1–44.
[22] H. Nie, S.-B. Hsu, J.P. Grover, Algal competition in a water column with excessive dioxide in the atmosphere, J. Math. Biol. 72 (7) (2016) 1845–1892.
[23] M.H. Protter, H.F. Weinberger, Maximum Principles in Differential Equations, Springer-Verlag, New York, 1984, p. x+261.
[24] S.-B. Hsu, P. Waltman, On a system of reaction-diffusion equations arising from competition in an unstirred chemostat, SIAM J. Appl. Math. 53 (4) (1993) 1026–1044.
[25] M. Ballyk, D. Dung, D.A. Jones, H.L. Smith, Effects of random motility on microbial growth and competition in a flow reactor, SIAM J. Appl. Math. 59 (2) (1999) 573–596.
[26] J. Balch, C. Guéguen, Effects of molecular weight on the diffusion coefficient of aquatic dissolved organic matter and humic substances, Chemosphere 119 (2015) 498–503.
[27] Y.C. Kim, Diffusivity of bacteria, Korean J. Chem. Eng. 13 (1996) 282–287.
[28] E.B. Kujawinski, J.W. Farrington, J.W. Moffett, Importance of passive diffusion in the uptake of polychlorinated biphenyls by phagotrophic protozoa, Appl. Environ. Microbiol. 66 (2000) 1987–1993.
[29] P.T.H.M. Verhallen, L.J.P. Oomen, A. Elsen, A.J. Kruger, The diffusion coefficients of helium, hydrogen, oxygen and nitrogen in water determined from the permeability of a stagnant liquid layer in the quasi-steady state, Chem. Eng. Sci. 39 (11) (1984) 1535–1541.
[30] A. Pazy, Semigroups of Linear Operators and Applications to Partial Differential Equations, Applied Mathematical Sciences, Vol. 44, Springer-Verlag, New York, 1983, p. viii+279.
[31] H.L. Smith, Monotone Dynamical Systems: An Introduction to the Theory of Competitive and Cooperative Systems, Mathematical Surveys and Monographs, Vol. 41, American Mathematical Society, Providence, RI, 1995, p. x+174.
[32] Y. Wang, J.P. Shi, J.F. Wang, Persistence and extinction of population in reaction-diffusion-advection model with strong allee effect growth, J. Math. Biol. 78 (7) (2019) 2093–2140.
[33] J.P. Shi, X.F. Wang, On global bifurcation for quasilinear elliptic systems on bounded domains, J. Differential Equations 246 (7) (2009) 2788–2812.
[34] J.P. Shi, J.M. Zhang, X.Y. Zhang, Stability and asymptotic profile of steady state solutions to a reaction-diffusion pelagic-benthic algae growth model, Commun. Pure Appl. Anal. 18 (5) (2019) 2325–2347.
[35] Y. Wang, J.P. Shi, Persistence and extinction of population in reaction-diffusion-advection model with weak Allee effect growth, SIAM J. Appl. Math. 79 (4) (2019) 1293–1313.
[36] N. Chitnis, J.M. Hyman, J.M. Cushing, Determining important parameters in the spread of malaria through the sensitivity analysis of a mathematical model, Bull. Math. Biol. 70 (5) (2008) 1272–1296.
[37] D.C. Coleman, C.V. Cole, H.W. Hunt, D.A. Klein, Trophic interactions in soils as they affect energy and nutrient dynamics. I. Introduction, Microb. Ecol. 4 (4) (1977) 345–349.
[38] P. Magal, X.-Q. Zhao, Global attractors and steady states for uniformly persistent dynamical systems, SIAM J. Math. Anal. 37 (1) (2005) 251–275.
[39] R.S. Cantrell, C. Cosner, V. Hutson, Permanence in ecological systems with spatial heterogeneity, Proc. R. Soc. Edinburgh A 123 (3) (1993) 533–559.
[40] J.K. Hale, P. Waltman, Persistence in infinite-dimensional systems, SIAM J. Math. Anal. 20 (2) (1989) 388–395.
[41] H.L. Smith, X.-Q. Zhao, Robust persistence for semidynamical systems, in: Proceedings of the Third World Congress of Nonlinear Analysts, Part 9 (Catania, 2000), Nonlinear Anal. 47 (9) (2001) 6169–6179.
[42] M.G. Crandall, P.H. Rabinowitz, Bifurcation from simple eigenvalues, J. Funct. Anal. 8 (1971) 321–340.
[43] P. Liu, J.-P. Shi, Y.-W. Wang, Imperfect transcritical and pitchfork bifurcations, J. Funct. Anal. 251 (2) (2007) 573–600.